INFORMATION TO USERS

This dissertation was produced from a microfilm copy of the original document. While the most advanced technological means to photograph and reproduce this document have been used, the quality is heavily dependent upon the quality of the original submitted.

The following explanation of techniques is provided to help you understand markings or patterns which may appear on this reproduction.

1. The sign or "target" for pages apparently lacking from the document photographed is "Missing Page(s)". If it was possible to obtain the missing page(s) or section, they are spliced into the film along with adjacent pages. This may have necessitated cutting thru an image and duplicating adjacent pages to insure you complete continuity.

2. When an image on the film is obliterated with a large round black mark, it is an indication that the photographer suspected that the copy may have moved during exposure and thus cause a blurred image. You will find a good image of the page in the adjacent frame.

3. When a map, drawing or chart, etc., was part of the material being photographed the photographer followed a definite method in "sectioning" the material. It is customary to begin photoing at the upper left hand corner of a large sheet and to continue photoing from left to right in equal sections with a small overlap. If necessary, sectioning is continued again – beginning below the first row and continuing on until complete.

4. The majority of users indicate that the textual content is of greatest value, however, a somewhat higher quality reproduction could be made from "photographs" if essential to the understanding of the dissertation. Silver prints of "photographs" may be ordered at additional charge by writing the Order Department, giving the catalog number, title, author and specific pages you wish reproduced.

University Microfilms

300 North Zeeb Road
Ann Arbor, Michigan 48106

A Xerox Education Company

73-4962

RICHTER, Clifford Wayne, 1945-
IN VIVO DOSIMETRY OF ^{99m}Tc LABELLED
AGGREGATES USED IN LUNG SCANNING.

The University of Oklahoma, Ph.D., 1972
Health Sciences, radiology

University Microfilms, A XEROX Company, Ann Arbor, Michigan

THIS DISSERTATION HAS BEEN MICROFILMED EXACTLY AS RECEIVED.

THE UNIVERSITY OF OKLAHOMA

GRADUATE COLLEGE

IN VIVO DOSIMETRY OF ^{99m}Tc LABELLED AGGREGATES USED IN LUNG SCANNING

A DISSERTATION

SUBMITTED TO THE GRADUATE FACULTY

in partial fulfillment of the requirements for the

degree of

DOCTOR OF PHILOSOPHY

BY

CLIFFORD WAYNE RICHTER

Norman, Oklahoma

1972

IN VIVO DOSIMETRY OF ^{99m}Tc LABELLED AGGREGATES USED IN LUNG SCANNING

APPROVED BY

Robert Y. Nelson

David W. Anderson

Larry Cantu

James M. Robertson

DISSERTATION COMMITTEE

PLEASE NOTE:

Some pages may have

indistinct print.

Filmed as received.

University Microfilms, A Xerox Education Company

ACKNOWLEDGEMENTS

The author would like to express his appreciation to Dr. Robert Y. Nelson, Dr. David W. Anderson, Dr. Larry Canter, Dr. James M. Robertson, and Dr. Edwin H. Klehr for their suggestions and assistance with this study.

The author wishes to express thanks to his loving wife, Delores, for her encouragement and understanding during the course of this endeavor.

A special thanks is extended to the Department of Radiological Sciences at the University of Oklahoma Health Sciences Center, and to Mr. Vernon J. Ficken for providing the facilities and the lung scanning agent for this research. I would, also, like to thank the U.S. Public Health Service for partial support of my graduate study.

This study was done in partial fulfillment of the requirements for the degree of Doctor of Philosophy from the University of Oklahoma.

TABLE OF CONTENTS

LIST OF TABLES

LIST OF ILLUSTRATIONS

IN VIVO DOSIMETRY OF ^{99m}Tc LABELLED AGGREGATES USED IN LUNG SCANNING

CHAPTER I

INTRODUCTION

Lung scanning is a screening procedure used to diagnose and locate pulmonary emboli. It is widely used in the United States at this time. To perform a lung scan, five millicuries of radioactive technetium-99m in the form of colloid particles are injected in the blood stream and collect in the lung.

In this study, we have measured the dose delivered to a dog lung during a lung scanning procedure in order to better evaluate dose to human lungs. Doses from diagnostic studies such as lung scans must be known with great certainty because of their widespread use. Diagnostic studies can contribute much more to overall radiation burden than the relatively small number of exposures in therapy.

The patient dose, due to various procedures involving radioactive isotopes, needs to be known with certainty in order to evaluate the benefits of the procedure vs. the radiation hazards. This evaluation may be very hard to accurately assess. Another factor to be considered is that when one uses scintillation imaging devices, it is desirable to use as much isotope as can be safely administered. The higher counting rates often give the best images. If the

true dose is very small, it may be possible in some cases to administer more isotope to obtain a better scan.

With the advent of thermoluminescent dosimeters of very small size, it is now possible to measure dose in areas that were unassessable by previous dosimetric methods. This study was undertaken to better evaluate the dose to the lung from technetium-99m labelled sulfur macroaggregates used in lung scanning. In it we compare the dose calculated by a well known procedure to the dose as measured with thermoluminescent dosimeters. To date, calculated doses have only been checked experimentally in phantoms, and in a few cases by dosimeters that have been surgically implanted at various locations in the body. The surgical implants have been in connection with therapy procedures (Boone, 1967).

The main feature of this study was that very small thermoluminescent dosimeters were injected into the blood stream and proceeded in a manner similar to the scanning agent to the lung vasculature. It had been found by Darnell (1967) that the dosimeters are more evenly spread through the lung than those that could be surgically implanted.

This study involved the use of dogs as experimental animals. The labelled lung scanning agent was first injected into the cephalic vein of the foreleg of the dog. Immediately after the particles were injected, the dosimeters were injected into the jugular vein. The dosimeters were then filtered out in the lung vasculature, but due to their relatively large size,

they were trapped in arteries before they reached the capillaries. Twenty four hours after injection, the dogs were sacrificed and the dosimeters recovered upon removal of the lung.

The in vivo dose, which was measured, will be compared to the calculated dose in a later section. Another study (Darnell, 1967), indicates that there is a large difference between the calculated and the measured in vivo dose. The possible causes of this discrepancy are investigated in a later section.

CHAPTER II

BACKGROUND OF LUNG SCANNING

In 1963 the first lung scans were carried out in man. The importance of lung scanning presents itself in the fact that nearly one-half of adults dying from all causes have pulmonary emboli present (Wagner, 1968). Pulmonary emboli are the most common of the serious disorders affecting pulmonary circulation. Pulmonary emboli may exist in a very serious form and not be properly diagnosed. Many emboli do not produce symptoms and are not detected, and in other cases produce symptoms that are very similar to other diseases and disorders (Wagner, 1968).

Pulmonary emboli usually originate as thrombi in the large pelvic veins, or less frequently, in the lower extremities. They usually occur as a result of being confined to bed because of surgery, pregnancy, or any condition that results in poor blood flow. As the patient regains circulation, the clots will migrate to the lungs or heart.

Lung damage results when a clot of sufficient size lodges in the lung vasculature that supplies that area of the lung. The body has several methods of breaking down emboli. This may be accomplished through anastomasis or by dissolving the emboli with proteolytic enzymes. If the emboli are not removed, parts of the lung, depending upon the supply from the artery, will cease to function. Emboli that remain trapped for 24 hours or more may cause serious

damage. Studies have shown that some emboli may remain trapped in the lung for as long as ten days (Duffy, 1968).

Pulmonary emboli are very difficult to diagnose and locate. To produce symptoms 30 to 50% of the capillary bed must be blocked (Wagner, 1968). Early symptoms may be falsely diagnosed as early pneumonia. Diagnosis of pulmonary emboli is complicated by the fact that X-rays can detect emboli in only about 20% of the severe cases (Wagner, 1968). Other diagnostic techniques such as pulmonary angiography can be hazardous and would not be desirable to use as a screening method.

The first lung scans were performed with macroaggregated albumin labelled with iodine-131 (^{131}I-MAA), which had a particle size range of 10 to 90 microns in diameter. The macroaggregated particles will break into smaller sizes upon injection and by blood flow against and around the particles in the capillaries of the lung (Duffy, 1968). The size range of the normal lung capillary has been found by Weibel (1963) to be one to 15 microns with an average capillary diameter of 8.2 microns.

When particles of this size range are injected intravenously, they act as small emboli and lodge in the lung capillaries in the portions of the lung that have unobstructed blood flow. If emboli are present, the area of the lung with the decreased blood flow will show up on the scan as an area of decreased activity, since the amount of labelled aggre-

gates filtered out is in direct proportion to the blood flow to the area. This provides the basis of the diagnostic test for pulmonary emboli.

Lung scans were first performed with rectilinear scintillation crystal detectors. This method of scanning has lead to an acceptable method of screening patients suspected of having pulmonary emboli. Later developments have improved the imaging methods. Stationary detector devices, referred to as cameras, have special advantages when all parts of the study field must be examined simultaneously.

The Anger camera was introduced in 1956 (Wagner, 1968). The device consists of a multi-hole collimator that projects the radiation image onto a 1/4 inch thick sodium iodide crystal. The crystal is viewed by an array of 19 photomultiplier tubes. The position of the light flashes is computed from information received from intensities from the various phototubes. The camera type imaging devices have nearly replaced the use of rectilinear scanners in many applications. This is due to the fact that cameras can view the entire area at once and get the information much quicker. Time is the main advantage of using the camera type imaging device.

In the past two years, technetium-99m has become the agent of general use. The main reason for the increased use of technetium is that the photon of the iodine-131 has

an energy of 363 KeV, and this energy has a low effieiency (21%) of interaction with the Anger camera crystal. On the other hand, the 1/4 inch thick crystal is 75% efficient for the 140 KeV photons of the technetium-99m. Another reason is that the dose to the lung is decreased by a factor of approximately ten when using the same number of mCi of technetium-99m as compared to iodine-131. The lower dose from technetium-99m is a result mainly of the six hour physical half-life and the lower amount of beta like emissions. The half-life of iodine-131 is 8.05 days, and the relatively large amount of beta is the major contributor to patient dose while contributing no medical information. The longer half-life of iodine-131, and the large amounts of beta emmissions contributes to a much higher dose than technetium-99m to get the desired results on the scintillation crystal.

The development of lung scanning agents now gives the physician a tool with which to observe patients in a situation that could lead to the formation of pulmonary emboli and then to begin specific treatments upon the early diagnosis. When pulmonary emboli are diagnosed, a program of very specific treatment can be initiated. The program involves the use of anticoagulant type drugs to prevent clot formation, proteolytic agents to dissolve any thrombi already formed, and various specific surgical techniques.

CHAPTER III

FATE OF THE LUNG SCANNING AGENT

Distributing particles in the lung to perform a scan involves the deliberate, but clinically safe, blockage of pulmonary capillaries by the labelled aggregates.

The agent is injected into the cephalic vein which flows up the arm and empties into the upper axillary vein. The upper axillary vein at the first rib becomes the subclavian vein, which passes medially to join the internal jugular and form the brachiocephalic vein on each side (inniminate vein). This then goes into the superior vena cava which dumps into the right atrium of the heart. Then it is moved into the right ventricle, which pumps the blood into the pulmonary artery. This artery branches and forms the pulmonary capillaries in which the scanning agent is filtered out, as the blood is being pumped through the lungs, while it is being oxygenated. The blood, without the scanning agent, after being oxygenated, returns to the heart in the pulmonary veins to the left atrium, then to the left ventricle to be pumped to all areas of the body through the aorta.

Posture and gravity has a marked effect on the distribution of the scanning agent in the lung (Tow, 1966). Particles are more uniformly distributed when the subject is in the supine position. In the standing position, the greatest fraction of the particles are found in the lower one third of the lung. Studies by Wagner (1968) also point out the blood flow was

higher on the downside lung when injecting a patient in the right or left decubitus position.

Five millicuries of technetium-99m using sulfur macroaggregates are used in the human lung scan. This preparation contains no more than 3 X 10^6 particles. Weibel (1963) states that there are approximately 300 X 10^6 precapillary segments larger than ten microns in diameter in the lung. This shows that little of the functional pulmonary area is blocked by the scanning agent.

Many of the aggregates undergo fragmentation and remain in the lung for only a few hours. The residence times (biological half-life) in the lung are affected by the rate of fragmentation, which can be caused by mechanical action of blood pressure. The physical mechanism of the blood flow against and around the particles in the blood vessels also causes some particles to break. Larger particles seem to take more time to clear the lung. This may be explained by the fact that they must fragment more to be cleared by the lung.

Miller (1970) has observed that sulfur macroaggregates may be removed by macrophages. The sulfur macroaggregates may be observed in macrophages as soon as 30 minutes after deposition of the scanning agent in the lung. The particles are engulfed by macrophages and dissolved by proteolytic enzymes (lysozymes). The fate of the sulfur colloid removed from the lung by the reticuloendothelial system is that it is ingested by the alveolar macrophages. The particles then

are first noted in the liver and the spleen. Since it has been found that the activity in the liver and the spleen decreases, it seems as if the sulfur is metabolized by the reticuloendothelial system.

The determination of the biological half-lives with a large degree of certainty is of great importance in the determination of the calculated dose to the organ. The biological half-life is the time required for the body to eliminate one-half of an administered dose of any substance by regular processes of elimination. Most half-life studies involve the use of scintillation counting over an organ. The area of highest concentration in the organ is located, and counts are made at certain times post injection. This data is then plotted relative to the initial counting rate to get the biological half-life.

Another method is to sacrifice laboratory animals at various times and remove the organs of interest. The organs are then counted separately to determine the remaining activity. This method takes into account the variability between animals. Both methods seem to produce similar results.

The fate of the macroaggregated albumin has been investigated by DeLand (1966). Particles with a size range of five to 100 microns, with 60% above 20 microns, were injected, and the half-life in the lung was found to be eight hours. The range of values in that study was from four to

twelve hours, indicating much variation. A second component was noted to have a half-life of 72 hours. A third biological elimination component has a half-life of 55 days. That study was accomplished using macroaggregated albumin labelled with iodine-131, so the first two components are most important in assessing lung dose. Due to the current use of macroaggregated albumin and sulfur colloid aggregates labelled with technetium-99m, the first half-life component of the particular agent used is highly important in calculating the lung dose. Very little of the dose is contributed after the first day when using an agent labelled with technetium-99m.

Biological half-life studies were conducted by Ficken (1970) on sulfur macroaggregates. This study used sulfur colloid aggregates labelled with sulfur-35 to find the fates of the particles. Sulfur-35, with an 87 day half-life, was long enough to allow following the particles much longer than if labelled with technetium of iodine. This study indicated that 70% of the original activity that was trapped in the lung was cleared with a biological half-life of six hours, 20% was cleared with a half-life of 22 hours, and the remaining 10% was cleared with a biological half-life of 400 hours. This clearance pattern is similar to the one for iodine-131 macroaggregated albumin, as was investigated by DeLand (1966).

These studies of biological half-life of the particles are very important in assessing the movement out of the

lung. Since very little of the lung function is compromised, it is of relatively little importance to know the residence times in the lung for this reason. However, as mentioned before, biological half-life changes will directly affect the radiation dose; therefore, it was very important to know them accurately for this study.

CHAPTER IV

LUNG ANATOMY

The lung contains three basic components; air, blood, and tissue. The tissue forms the basic constraints for the blood and the air. Certain tissue allows a gaseous exchange through it. The arrangement of the airways and blood vessels of the lung branch at the central area of the lung. Functionally the center of the lung is located at the area where the airways terminate in the alveoli and come in close relationship with the capillary network. The right and left main pulmonary arteries begin at the bifurcation of the pulmonary arterial trunk. This arrangement is generally in the form of a fan and continues until it terminates in the alveolar sacs.

In the mature lung, airways and blood vessels have a characteristic relationship to each other. This is shown in figure 4.1. The pulmonary arteries are seen to accompany the bronchi quite closely. The pulmonary veins have a greater variation, but tend to be between the airway tree. This arrangement is maintained throughout the lung, from the hilum to the periphery (Bloomer, 1960).

Systemic capillaries are rather long thin tubes that are connected to smaller capillaries to form a dense network of alveolar capillaries. These in turn form a very dense capillary network in the alveolar wall. The capillaries

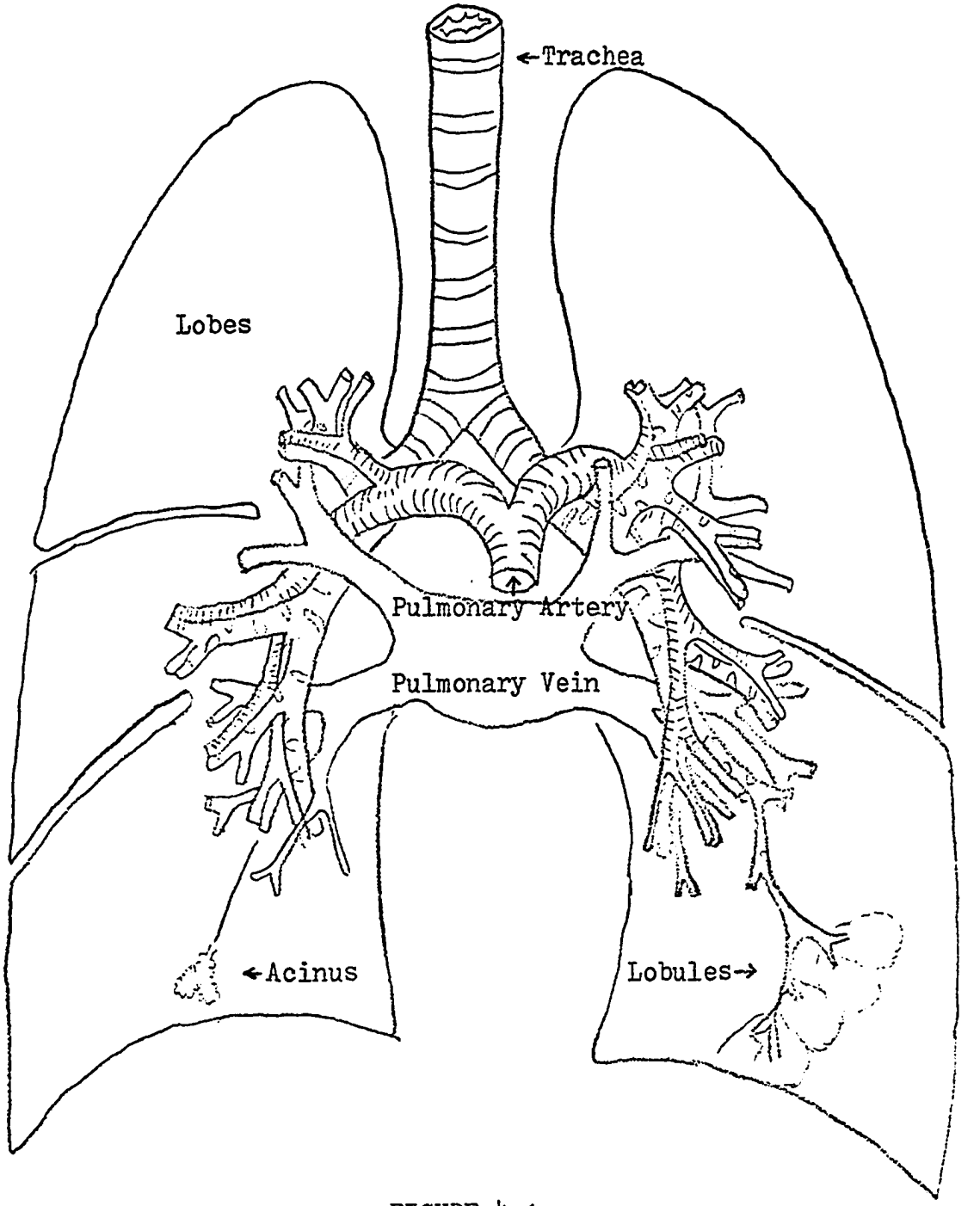

FIGURE 4.1

The Lung

have an internal average diameter of 8.2 microns with an external diameter between one and 15 microns. Weibel (1963) has found the basic number of capillaries in the human lung to be 280×10^9. This number is nearly independent of the lung size.

There are 300×10^6 alveoli in the lung. This means that each alveolus is surrounded by 1,000 to 2,000 capillary segments. The capillary network can be described as a continuous and large vascular sheet with an area of 35 to 40 square meters.

Generally, it was found that differences between species are not qualitative but quantitative (Weibel, 1963). It has been found that between species the lung volume is proportional to body weight i.e., the lung weight and volume are related by density, therefore, the lung weight is a constant fraction of body weight. This has been shown by Tenny (1963) and is summarized in figure 4.2.

Tenny's study has shown that the lung volume is a direct function of body weight and not a direct function of metabolic rate. The line in figure 4.2 approximates a straight line with a slope of 1.02. It has been found that the metabolic rate correlates with body weight to the 0.74 power. The total respiratory frequency does correlate to the metabolic activity to the inverse of the body mass to the 0.28 power (Adolf, 1949). The number of alveoli per unit volume of lung is higher in animals with a greater

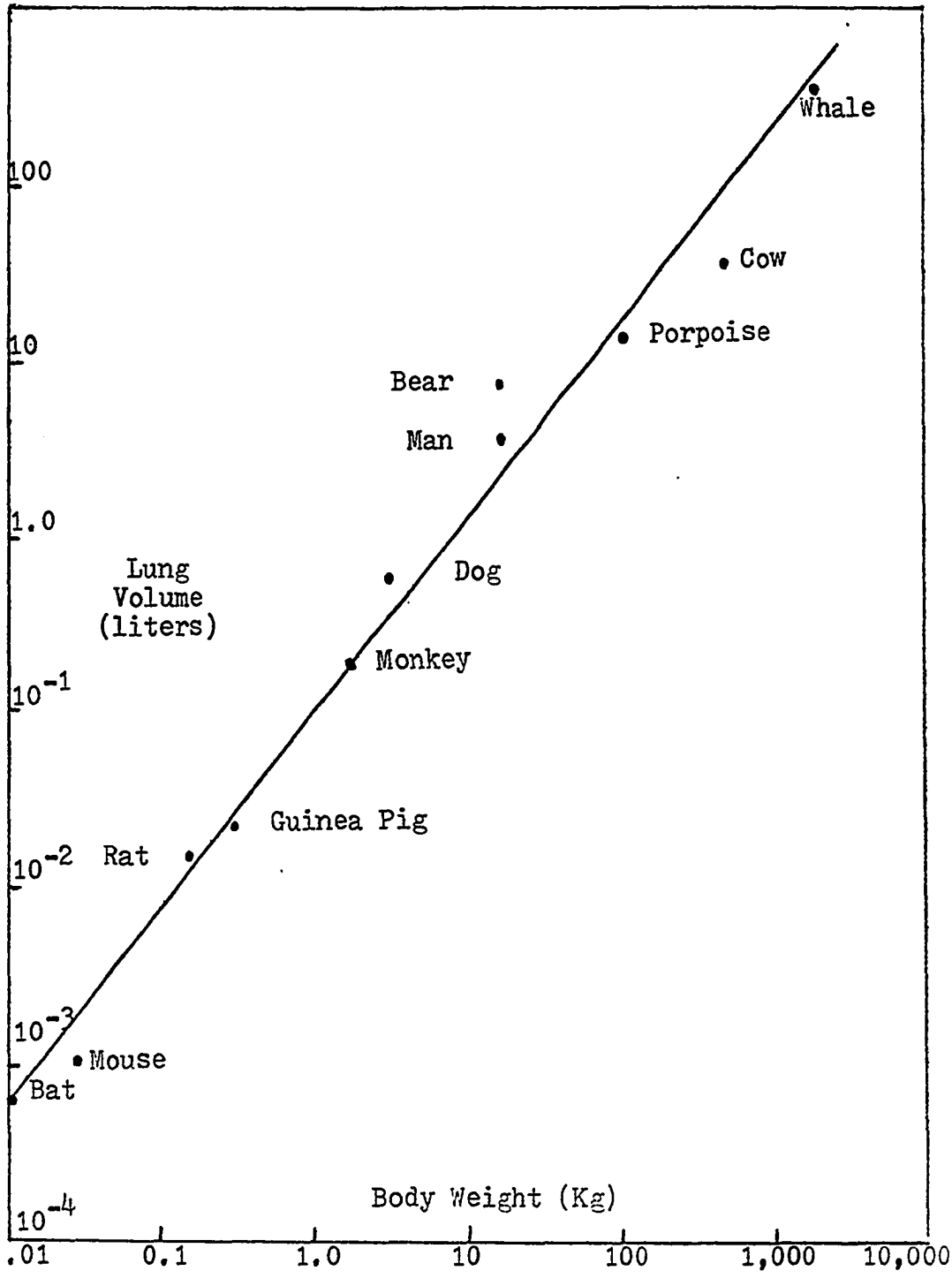

Figure 4.2 Logarithmic plot of lung volume vs. body weight (Tenney, 1963)

metabolic activity (Tenny, 1963).

It can be seen from the study of Tenny (1963) that the lung weight is approximately 1.4% of body weight. There seems to be quite a bit of uncertainty in this number. Much of the variance is due to the way that the lung weight was measured at autopsy. It has been found that when the lung is removed and the large vessels are cut, much of the blood is lost from the lung. This would tend to cause a lower value than actual live weight. The type of death that is encountered will change the amount of blood that is left in the lung (DeReuck, 1962). Death by electrocution will actually force blood from the lung, and death by anesthesia will cause a larger amount of blood than normal to accumulate in the lung.

Typer (1967) reports that there is very little in the literature concerning precise information on comparative anatomy of the lung among various species of mammals. The main discrepancies between man and dog are in the delineation of the secondary lobes according to his study. It was also found that there were some differences in the blood vessels supplying the lung, but this was not in areas that would affect this dosimetry study.

For the standard, 70 kilogram man, the lung weighs 1,000 grams which is 1.4% of body weight (Snyder, 1969). The human lung is composed of three lobes on the right and two lobes on the left.

Ross (1957) has found differences between the dog and man's bronchial tree architecture. This would probably be expected due to the difference in the number of lobes. The dog lung consists of four lobes on the right which carries 53.9 to 62.2% of the total blood flow. The left lung has three lobes and has 37.8 to 46.1% of the total blood flow to the lungs of the dog. Taplin and Poe have made these regional blood flow studies (Darnell, 1967). It would be expected that the labelled aggregates and the injected dosimeters would follow similar patterns as the blood. In the dog lung, blood is distributed with 38% in the capillaries, 27% in the arteries, and 35% in the veins (DeReuck, 1962). This shows that the lung has a large amount of blood in the area where respiration is taking place.

Although there are definite gross changes in the lung structure between the human and the dog lung the changes at the level of capillary size and general distribution of pre-capillary segments are slight. In any case, dogs are the most often used experimental animal in respiratory studies as noted by Schmidt (1961). In physiological studies, 70% of all animals used are dogs.

The main cause of concern in a dosimetry study of this type is not general lung architecture, but of a uniform distribution of both the scanning agent and the dosimeters in the volume occupied by the lung. This condition should be met because lung scans of dogs by Ficken (1970) indicate a uniform aggregate distribution. If the aggregates are

distributed evenly, due to the large number of precapillary segments, the dosimeters, also, should be evenly distributed.

It is interesting to note that due to the differences in size of the dosimeter and the labelled aggregate, the two will not be in direct contact. This is because the aggregates will go much deeper into the capillaries than the relatively large dosimeter. The closest contact that can be made is one that would be in juxtaposition, with the thickness of the capillary wall and the lung epithelium separating them.

It must be remembered in any study using animals, that the individual variations amoung subjects can add a source of error that is very difficult to analyze (Cass, 1961). A more comprehensive treatment of the morphometry of the lung has been written by Weibel (1963) and the author refers you to this work for more information.

CHAPTER V

THERMOLUMINESCENT DOSIMETRY

5.1 Physical Process

Thermoluminescent dosimetry is rapidly becoming one of the most common methods of measuring dose due to ionizing radiations. A description of the physical process of thermoluminescence is background information in a study of this nature since thermoluminescent materials are used as the dosimetry system.

The fundamental theory of thermoluminescence is not fully known, but the physical process is qualitatively understood. For a detailed discussion of thermoluminescent dosimetry, one is referred to the works of Fowler and Attix (1966) and Cameron (1968). An outline of thermoluminescence is given for the readers convenience.

As ionizing radiation interacts with matter, the predominant processes are ionization and excitation of the orbital electrons. In a compound such as lithium fluoride, the ionized electrons and the associated free holes can be trapped in a metastable energy state in the crystal. These traps are at the sites of defects in the crystal lattice. The electrons and the holes are held by the Coulomb's force to the lattice defects. The electrons and the holes can escape the traps and the probability of escaping the traps is dependent upon the temperature. If the energy difference between the metastable state and the energy bands is large

enough, the traps will only be emptied at elevated temperatures. This is the case with lithium fluoride, for which the energy difference between the valence band and the conduction band is about 12 eV.

The temperature necessary to empty the traps will be determined by the difference in energy between the trap and the conduction band. This is on the order of a few eV. When the trap is emptied at a temperature that is higher than room temperature, i.e., thermally excited, this causes the electron-hole pairs to return to ground state. Thermoluminescence occurs when the electrons trapped at the anion vacancies recombine with the holes. In the process of returning to the ground state, a characteristic light is given off. This thermally stimulated production of light is known as the process of thermoluminescence. A schematic of the processes involved in thermoluminescence dosimetry is shown in figure 5.1.

A plot of light output vs. temperature, showing the luminescence peaks is called a glow curve. As the temperature of the phosphor is increased by heating, the probability of release of electrons from a metastable state increases, when the temperature reaches the required level, one level of metastable state traps will empty and give off a characteristic light. As the temperature continues to rise, other metastable traps will empty with additional light peaks. It has been found that there are five such peaks

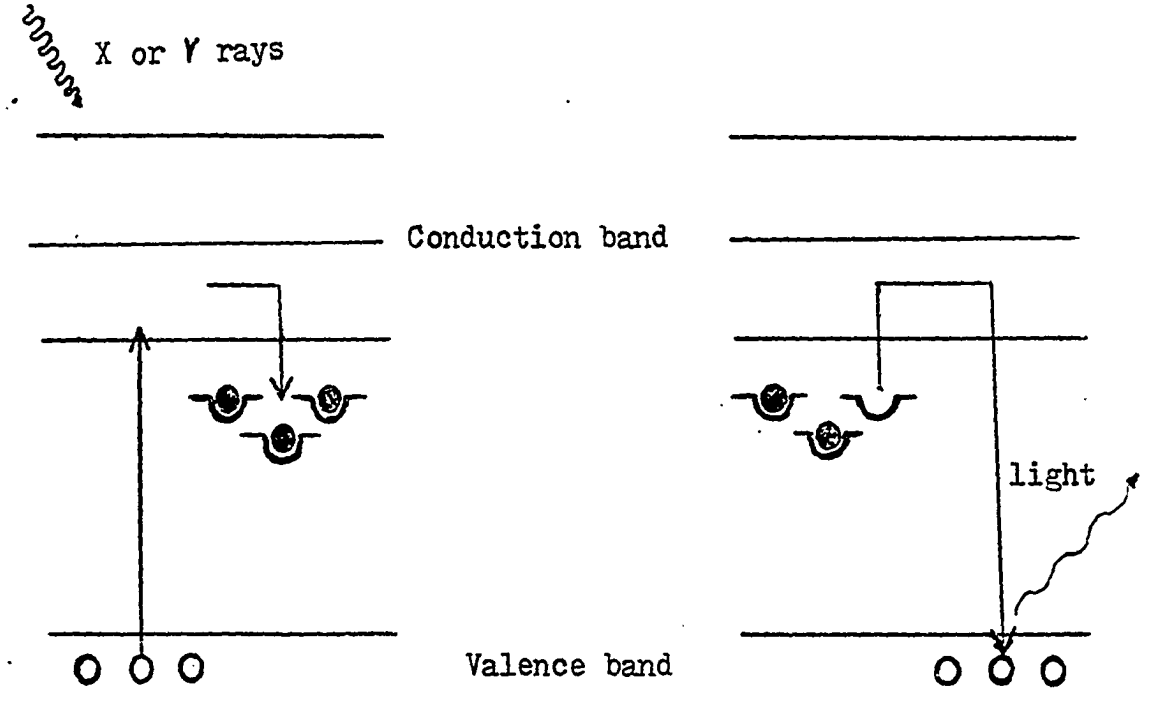

a) Irradiation b) Heating

Figure 5.1 Processes involved in thermoluminescence dosimetry

(a) Irradiation produces free electrons and holes. The electrons are free to travel through the solid in the conduction band until they are either trapped (black dots) or fall back into the valence band with the emission of light.

(b) On subsequent heating the trapped electrons are given sufficient thermal energy to escape from the traps, and upon return to the valence band (and recombination with a hole) they emit light. (Attix, 1966)

for lithium fluoride. A typical glow curve is shown in figure 5.2 for lithium fluoride. Zimmerman (1966) has found that after irradiation, the five lithium fluoride peaks will decay exponetially at room temperature, with the following half-lives; peak one... five minutes, peak two... ten hours, peak three... one half year, peak four... seven years, and peak five... eighty years.

The rate at which thermoluminescence is released from lithium fluoride is dependent upon the temperature. The thermoluminescent energy loss of the main glow peak is about five percent per year at room temperature. The loss is increased to about 15% at body temperature. These losses were noted by Cameron (1964). Due to these relatively small losses of thermoluminescence at body temperature, studies that involve only a few days to complete do not need to be corrected for decay.

5.2 Energy Dependence

The effective atomic number of lithium fluoride is 8.14. This compares with 7.64 for air and 7.42 for tissue. At energies above a few hundred KeV the ratios of the mass absorption coefficients for lithium fluoride, air, water, and tissue vary relatively little with photon energy, so the lithium fluoride dose response can be considered a very close approximation of the dose received by equal volumes of these materials exposed under similar conditions.

At photon energies of the range of 25 KeV and lower,

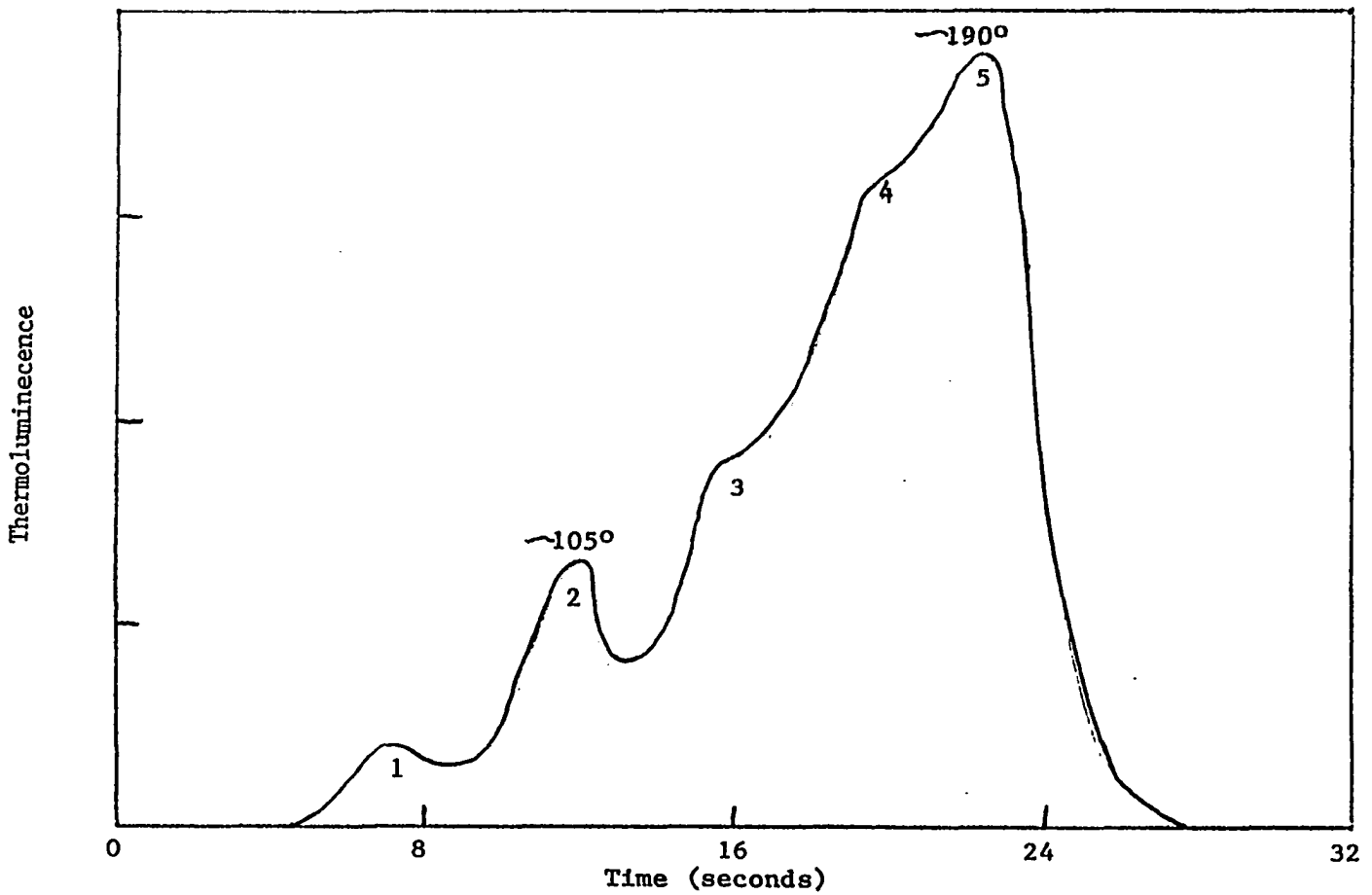

Figure 5.2 Typical glow curve of LiF (Zimmerman, 1966)

the photoelectric energy absorption process predominates and is heavily dependent upon the atomic number of the media. This means that the Z number, is the important factor in radiation interactions below 25 KeV. Since lithium fluoride has a higher Z number that tissue, it is known that there is a marked energy dependence in the range of radiation energies encountered in this project. Cavity theory would predict some over response at energies below 100 KeV as compared to cobalt-60 photons (Cameron, 1968). The lower energy characteristic X-rays of technetium-99m may over respond by 35%. Increased response will also be the case for degraded 140 KeV photons of technetium-99m. A graph of the response of lithium fluoride vs. photon energy is shown in figure 5.3 (Cameron, 1968).

Due to this energy dependence in the dosimeter response, it will be necessary to calibrate the dosimeters directly against technetium-99m and cobalt-60. Cobalt-60 is customarily used as a standard for calibration.

5.3 Instrumentation

The lithium fluoride dosimeters are read in a thermoluminescent dosimeter reader. The instrument is essentially a light measuring device that supplies controlled heat to the dosimeter.

To read the dosimeter, it is placed in the silver heating pan of the reader. When the heating cycle is started, it will heat, but not record the low peaks that contain no

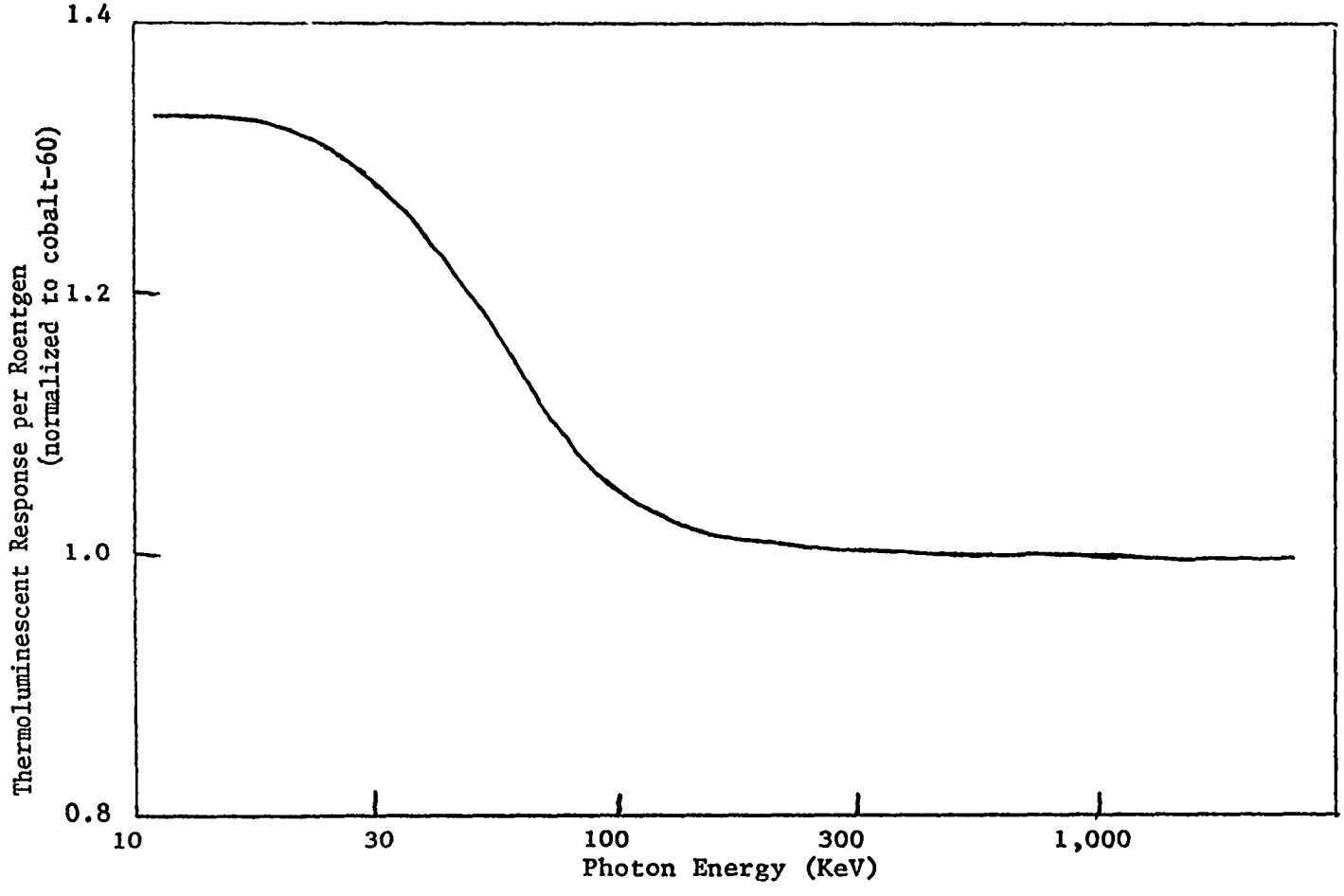

Figure 5.3 Thermoluminescent Response of LiF Below 1.2 MeV.

useful information. This is called a preheat cycle. When this portion of the cycle is complete, the temperature is quickly raised to the readout temperature. The reader will then record the light output from the higher energy traps. This light is sensed by the photomultiplier tube and is converted to current. This current is then converted to pulses which are integrated over the readout time and registered on the readout display. Such an operational procedure assures that only the more stable, higher temperature peaks are used for assessing dose. The heating cycle used was the cycle that was recommended by the manufacturer for lithium fluoride and is shown in figure 5.4.

For low background measurements, it has been found by Ailken et al. (1967) that oxygen tends to increase the counting rate. This is due to surface traps and oxygen holding the electrons in a stronger bond. This will cause traps that should have been emptied in the preheat cycle to empty at the higher temperature peak causing the readout to be higher than expected.

To minimize this effect, a nitrogen purge is recommended for low dose measurements. The manufacturer recommends that a nitrogen purge of 0.5 liters per minute be used for dose readouts below ten rads. In this study, the dosimeters were encapsulated in glass, therefore, the nitrogen purge was unnecessary.

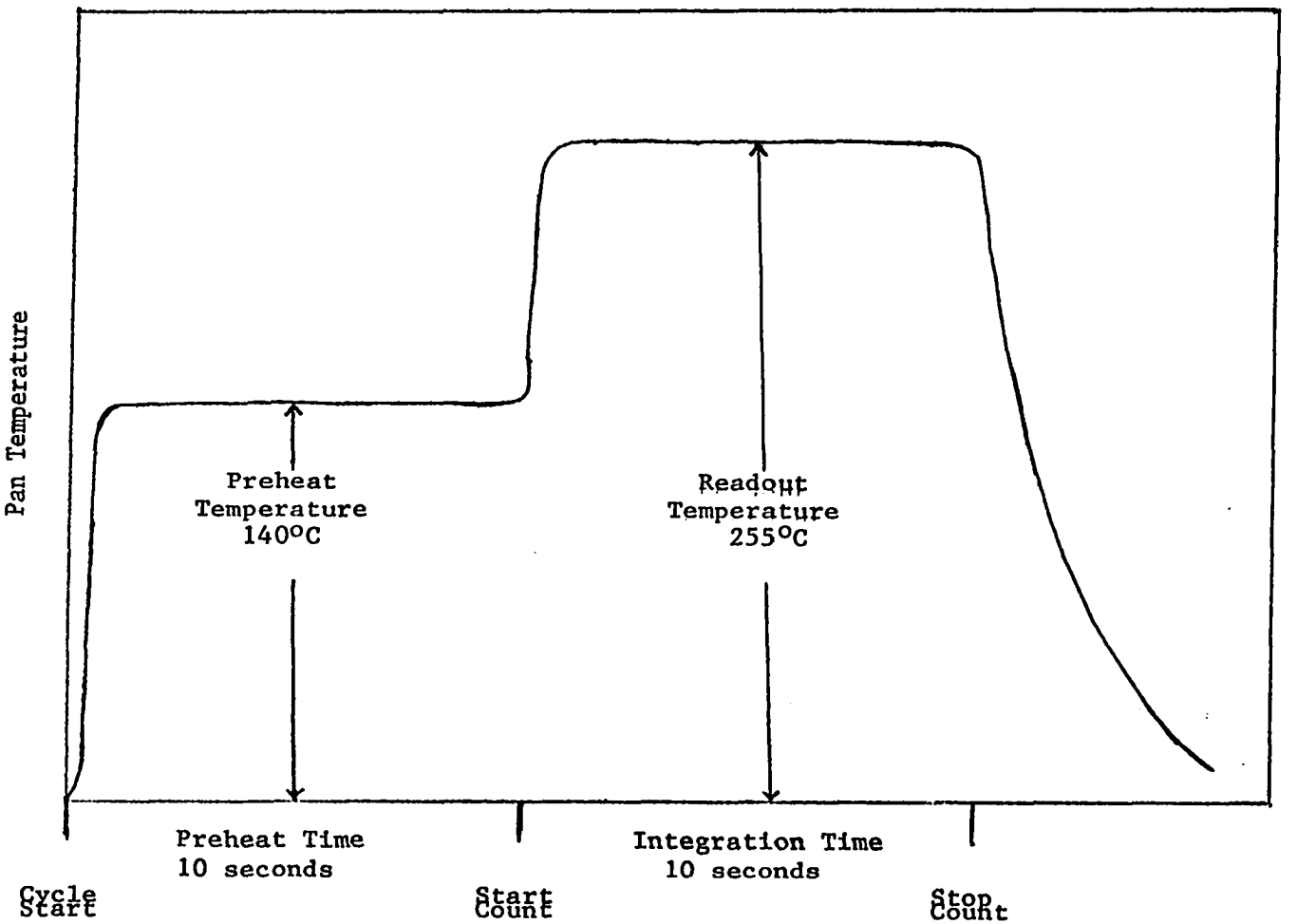

Figure 5.4 LiF Readout Cycle for Model TLR-5 Thermoluminescent Dosimeter Reader (Eberline Inst. Co., 1969)

5.4 Annealing Procedures

Most annealing procedures have been derived from the work of Zimmerman et al. (1966) and Cameron (1968). Pre-irradiation annealing cycles that have gained wide acceptance are to place the dosimeters in an oven for one hour at 400 $\pm$ 25°C. This will empty all of the traps in the phosphor. The dosimeters are then removed from the oven and allowed to cool for 20 minutes at room temperature. The next step of the annealing procedure arranges the traps so the 190°C peak will predominate. This step places the dosimeters in an oven for 24 hours at 80 $\pm$ 2°C. At the end of this time period, the dosimeters are cooled to room temperature and used.

A faster cycle has been developed by Beck (1968). It has the advantage of essentially the same sensitivity with less time. His procedure consists of placing the dosimeters in an oven at 400°C for 15 minutes, then cool to room temperature for 15 minutes, and then place the dosimeters in an oven at 100°C for two hours. This cycle arranges the traps in a manner similar to the previously mentioned cycle.

To anneal out the low temperature peaks before readout, a 140°C pre-heat cycle is used. This pre-heat cycle is recommended by Eberline Instrument Company specifically for lithium fluoride.

5.5 Cavity Theory

The measurement of energy absorbed in matter that is

exposed to radiation necessitates the introduction of a measuring device in the medium. In practice, this device is different in both atomic number and density from the medium, so it will create a discontinuity, which is referred to as a cavity. Cavity theory development has been summarized by Burlin (1968). The theory was developed assuming that the cavity dimensions were either small or large as compared to the range of the secondary electrons.

Berger (1971) has calculated the 90 percentile range for electrons in water. For 140 KeV electron, the range in water is 0.187 mm. The average secondary energy would be much less than this, and the corresponding range, then, would be greatly reduced. The dosimeter used in this study has a diameter of 0.8 mm and is 6 mm in length. Therefore, for radiations from technetium-99m, the dosimeter cavity is large as compared to the range of the secondary electrons. This means that the relative contribution to the total energy is small from the areas lying close to the boundary. For the rest of the cavity, the energy absorption is due to the properties of the cavity material only.

In the case of gamma rays, energy absorption in the cavity is due to the mass energy absorption coefficient of the cavity $(\mu_{en}/\rho)_c$. The absorbed dose in the medium also is proportional to the mass energy absorption coefficient of the medium $(\mu_{en}/\rho)_m$.

The increase in the value of the mass energy absorption coefficient, with decreasing energy for lithium fluoride, is greater than the increase in the mass energy absorption coefficient for tissue. This is due to the higher atomic number of lithium fluoride than tissue. This will lead to an over response of lithium fluoride that is not linear with decreasing energy.

CHAPTER VI

ABSORBED DOSE CALCULATIONS

6.1 Introduction

The calculation of absorbed dose may be accomplished by various methods. Many of the methods are seemingly different. Smith (1965) has done much work in the area of absorbed dose calculations. He states that the techniques using absorbed fractions are more reliable than other methods used in assessing absorbed dose.

Figure 6.1 shows the complicated spectra of radiations emitted by technetium-99m. Due to the numerous radiations, it is extremely difficult to arrive at an easily calculable method of assessing the absorbed dose. The MIRD method of calculating the absorbed dose takes into account 20 radiations that contribute to dose from technetium-99m and are noted in table one.

The method used in this study was the method of using the absorbed fraction as described by Loevinger and Berman (1968). These reports have been condensed by Smith et al., into the Medical Internal Radiation Dose Committee (MIRD), which are published as supplements to the Journal of Nuclear Medicine.

The photon absorbed fraction (ϕ) is the fraction of the emitted photon energy absorbed in the region of interest. The absorbed fraction is specific for the source, the absorber geometry, the photon energy, and the intervening material.

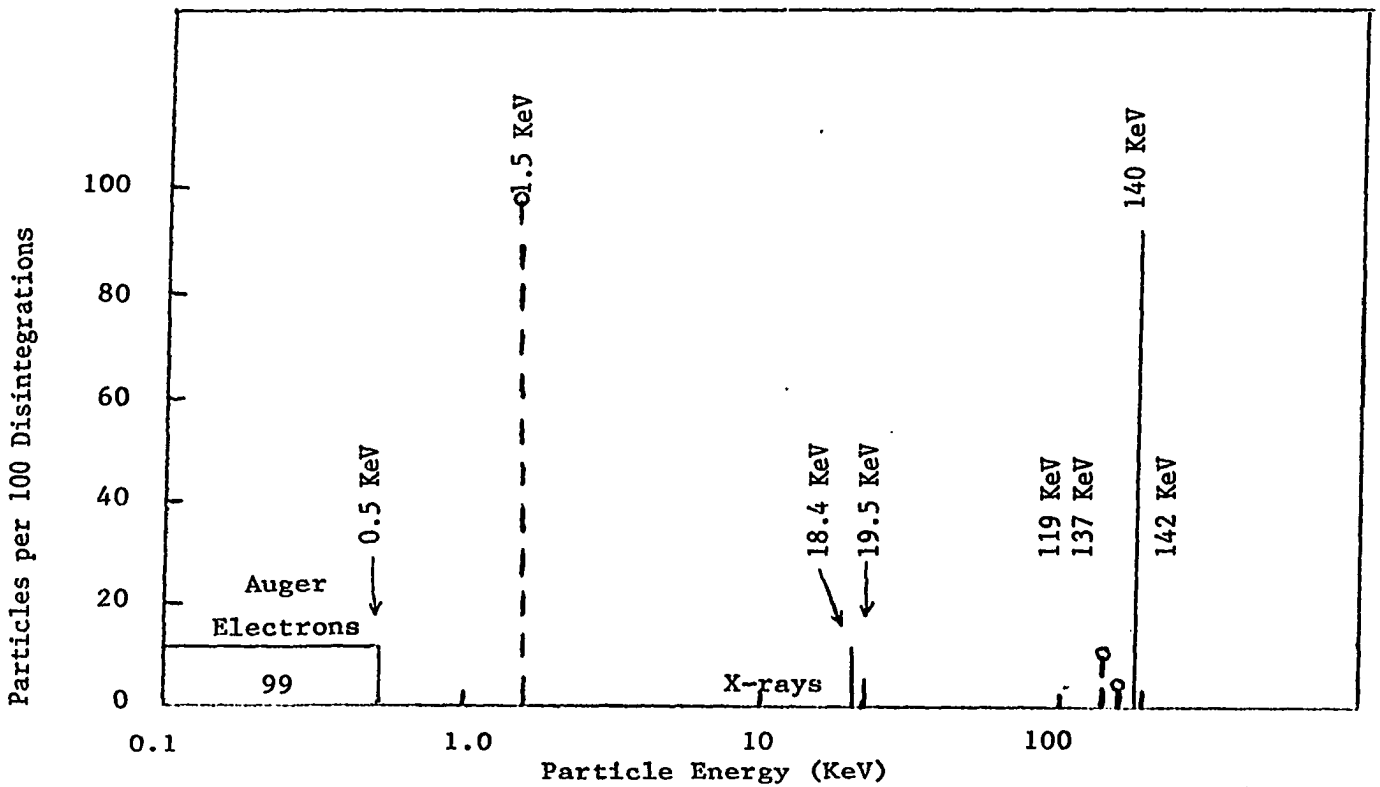

Figure 6.1 Spectrum of the radiation emitted in the decay of technetium-99m Electron lines are dashed and capped with open circles. Photons are solid lines. Many X-rays have been omitted for the sake of clarity. Auger electrons have line spectra that are crowded closely in the low-energy region of the spectrum.

Table 1. Values to calculate the total lung dose for ^{99m}Tc

Mean Energy MeV	Δ_i	ϕ	$\Delta_i \phi$
0.0021	0.0000	1.0000	0.0000
0.0017	0.0036	1.0000*	0.0036
0.1405	0.2643	0.0496	0.0131
0.1195	0.0225	1.0000*	0.0225
0.1377	0.0032	1.0000*	0.0032
0.1401	0.0011	1.0000*	0.0011
0.1427	0.0001	0.0496	0.0000
0.1217	0.0025	1.0000*	0.0025
0.1399	0.0009	1.0000*	0.0009
0.1423	0.0003	1.0000*	0.0003
0.0184	0.0017	0.5100	0.0009
0.0184	0.0008	0.5100	0.0004
0.0206	0.0005	0.4750	0.0002
0.0210	0.0001	0.4750	0.0000
0.0024	0.0000	1.0000*	0.0000
0.0155	0.0005	1.0000*	0.0005
0.0178	0.0002	1.0000*	0.0002
0.0202	0.0000	1.0000*	0.0000
0.0019	0.0004	1.0000*	0.0004
0.0004	0.0010	1.0000*	0.0010
		$\sum \Delta_i \phi$	= 0.0508

*Beta like components, $\phi = 1$

Data from Dillman (1969) & Snyder and Ford (1969) MIRD

The absorbed fractions for the MIRD work are calculated by means of Monte Carlo techniques. The technique utilizes equations for photon scattering and absorption as a probability distribution. A computer sampling is followed through 40,000 to 60,000 interactions in the material of interest. The absorbed fraction is obtained by adding the energy that has been lost in various target volumes. A through discussion is given by Brownell (1968).

6.2 Lung Dose Calculation

The presence of the scanning agent in the lung results in a dose to the lung, thus, we have a case of self irradiation. The formula for self irradiation is:

$$\bar{D}\ (\ v \leftrightarrow v) = \tilde{C}_v \sum_i \Delta_i \phi_i (v \leftrightarrow v) \qquad \text{rad}$$

Where:

$\bar{D}\ (v \leftrightarrow v)$ Mean absorbed dose (rad) the target volume, v, receives from the source distributed in the target volume, v.

$\tilde{C}$ Cumulated concentration of the activity in volume, v, in μCi-hr/g.

Δ_i Equilibrium absorbed dose constant for radiation of type i, where i = 1,2,3,..., with a fractional frequency n_i per disintegration, and a mean energy, $\bar{nE}_i$, in million electron volts per disintegration. $\Delta_i = 2.13\ n_i \bar{E}_i$ g-rads/μCi-hr. 2.13 is a units conversion factor.

$\phi_i (v \leftrightarrow v)$ The photon absorbed fraction or the quotient of the energy from the i^{th} type of radiation in the source, v, absorbed in volume, v, divided by the energy of the i^{th} type of radiation emitted by the source in volume, v.

The data in table one is the output data of all the 20 different energies of radiation that are given off in the decay of technetium-99m. Table one shows that the beta like components contribute 2.48 times as much dose as does the photons. This was found by a ratio of the absorbed fractions of the beta component compared to the gamma component. The photon dose is 28.7% of the total lung dose.

The calculation of the dose to the human lung from technetium-99m is demonstrated in the following example. The calculation is for standard man weighing 70 kilograms. The lung weighs 1.4% of body weight or 1,000 grams. The lung has a density of approximately 0.3 grams per cubic centimeter. The methods of the Medical Internal Dose Committee (MIRD) of the Society of Nuclear Medicine are used to calculate the dose to the lung from a technetium-99m labelled scanning agent. It was assumed that there was a 100% uptake by the lung of the scanning agent.

Ninty-five percent of the beta like emissions from technetium-99m are stopped in 0.0321 cm. This would indicate that very little of the beta like component would escape the lung and the assumption that $\phi = 1$ is, therefore, valid.

To solve for the cumulated concentration, the following equation is used:

$$C(t) = \int_{t_2}^{t_1} C(t) \; dt \quad \mu Ci/g$$

Where;

$C(t)$ The concentration in μCi/g, of the radionuclide in the tissue at anytime, t, in hours, for which the absorbed dose is being calculated.

t_2-t_1 The time interval (in hours) for which the absorbed dose is being calculated.

$$\hat{C}(t) = \int_0^\infty C(t)\,dt = 1.44 \sum_j C_j(0)\, T_{j_{eff}} \ \mu\text{Ci-hr/g}$$

Where;

$C_j(0)$ Initial concentration in μCi/g.

$T_{j_{eff}}$ Effective half-life of agent in hours.

If we assume that the biological half-life is large as compared to the six hour half-life of technetium-99m, then the effective half-life approaches six hours. The effective half-life is found by the following equation:

$$T_{eff} = \frac{T_{phy} \times T_{bio}}{T_{phy} + T_{bio}}$$

This assumption would lead to the largest possible dose to the lung. In effect, we assume that the isotope activity decreases only by radioactive decay and not by the biological removal processes, such as break-up of the particles followed by their removal by blood flow or other biological processes.

Studies by Ficken (1970) and others indicate that the biological elimination rate for sulfur colloids is on the

order of six hours. This rate is noted for the removal of 70% of the aggregates. The six hour component of the half-life study, which lasts for 72 hours is the most important, bacause little of the dose would be received by the lung after this time.

For the case of the six hour effective half-life:

$$\tilde{C} = 1.44 \times 1\mu Ci/g \times 6 \text{ hr} = 8.64\ \mu Ci\text{-hr/g}$$

This gives us all the information to substitute into the dose equation to calculate the lung dose for the case of the six hour effective half-life.

$$\bar{D}\ (v \leftrightarrow v) = \tilde{C} \sum A_i \phi_i (v \leftrightarrow v) = 439 \text{ mrad/mCi}$$

If we assume a six hour biological half-life, the effective half-life would now be three hours and the dose to the lung will be one-half as mu ch since the effective half-life substitutes directly in the dose equation. The dose for the three hour effective half-life to the lung is 219 mrad/mCi. The value of 219 mrad/mCi agrees very well with the value derived by Ficken (1970) of 210 mrad/mCi. He made his calculation using more classical equations.

6.3 24 Hour Dose Calculation

In this section, the basic equation used to calculate the dose will be modified to give a dose to the lung of standard man for a period of 24 hours after the injection. The calculation will be made to get a percent of infinite dose. Note that, when t = 24 hours and T_{eff} = 3 hours, the

fraction of the activity undergoing decay is equal to;

$$\left(1 - e^{\frac{-0.693 \times t}{T_{eff}}}\right) = 1 - e^{-5.55} = 0.996$$

Thus, after eight effective half-lives, very little activity is left, and the remaining possible dose is very small. In fact, 99.6% of the total dose is given during the first 24 hour period. The dose during the 24 hours period would be 218 mrad/mCi.

CHAPTER VII

EXPERIMENTAL DESIGN

7.1 Choice of Dosimeter

Several forms of thermoluminescent dosimeters were considered for this study. Lithium fluoride high sensitivity rods made by Harshaw Chemical Company (TL-100) were considered first due to the high precision at low dose. They measure 1 X 1 X 6 mm. Their main disadvantage is that they are soluble in water to the extent of 2.7 grams per liter of water. The surface etching caused by their solubility destroys some of the light emission properties and leads to poor reproducibility. Spuring (1971) is working on the use of lithium fluoride powder in aqueous solutions. There are still several problems involved in recovery, and at present these results would not be applicable to a study in biological systems. Even if all the problems in Spuring's study could be solved, their use in biological systems would be precluded by the toxicity of the lithium fluoride to biological systems.

Due to these problems, the dosimeters would need to be encapsulated to prevent their coming into direct contact with body fluids. After encapsulation, the size of the Harshaw TL-100 rods would be 2 X 7 mm. In order to be carried as far as possible into the pulmonary arteries, a small dosimeter was desirable. For this reason, the encapsulated rods were eliminated in favor of a smaller dosimeter. This was allowable

since the planned doses in the study were to be of the order of ten to twenty rads to the lung. Doses in this range are relatively easy to measure, even with very small dosimeters.

At this stage of dosimeter investigation, the micro-dosimeter made by Edgerton, Germeshansen, and Grier, Inc. (E G & G) was considered. These dosimeters contain 0.25 milligrams of lithium fluoride dosimeter grade powder encapsulated in glass. The glass has a wall thickness of 0.18 mm. The micro-dosimeter measures 0.8 mm in diameter and is 6 mm in length. This small size was very desirable due to the ease of injection, and increased penetration into smaller arteries in the lung. The more arteries utilized, the better will be the distribution of the dosimeters through the lung. The main sacrifice was for high precision at low dose measurements. These microdosimeters are capable of measuring one rad $\pm$ 20%. Since the planned doses were much more than one rad, the accuracy was considered sufficient. The magnitude of other variations usually encountered in biological experiments of this nature is likely to be more significant than dosimeter variation.

7.2 Dosimeter Calibration

Since thermoluminescent dosimetry is not a system of absolute measurement, but only a measure of relative responses, a system of comparison of the measured dose to a known dose must be made. The best method is to expose a portion of the batch to a known dose of radiation and obtain an average calibration factor for the entire batch.

The standard used for calibration was a cobalt-60 teletherapy unit. To calibrate the dosimeters, 25 were placed in a phantom and exposed using a 10 X 10 cm field at 80 cm SSD (source to skin distance) for a known period of time. The exposure used was approximately 50 roentgens. Appropriate roentgen to rad conversion, backscatter, and percent depth-dose factors were used to convert to dose in rads (Johns, 1969). Readout gives an average response in TL (thermoluminescent) units per cobalt-60 dose. An example of a calibration is given in the appendix, Table A.

Since a marked energy dependence has been noted for lithium fluoride in the energy range of technetium-99m, it was necessary to obtain directly the ratio of the technetium-99m response per rad to the Co-60 response per rad. It should be noted that the 0.18 mm glass wall should exclude all the beta like radiations of ^{99m}Tc as the range for a 0.12 MeV kinetic energy electron is 0.09 mm. This means that only the gamma dose would be measured.

The dosimeters were calibrated directly in a solution containing a known amount of technetium-99m. The activity of the ^{99m}Tc used in this experimental procedure was measured by a Mediac II dose calibrator. This instrument has a stated accuracy of better than one percent. The instrument was calibrated daily with a standard radium source. Factors were also used to correct for syringe fill and size.

The need for direct calibration is apparent, due to

cavity theory predictions of a small over response at 140 KeV, as compared to cobalt-60 photons (Cameron, 1968). The lower energy characteristic X-rays and degraded photons present in a material will lead to an even higher over response. The increased response at low energies (20 KeV) is 35 to 40% higher than for cobalt photons.

To calibrate the dosimeters with ^{99m}Tc, a cylinder of plexiglass was constructed, having a radius of five cm, and a height of 20 cm. The volume of this cylinder was 1570 ml. Volumes of one-half and one-quarter this size were also used by reducing the fluid height in the cylinder. The dosimeters were held at the central point of the cylinder by cellophane tape. These are standard sized cylinders for which values of the absorbed fractions have been calculated using a Monte Carlo computer program and published by MIRD (Brownell et al., 1968).

The absorbed dose delivered at the central point of a target containing a uniformly distributed source is greater than the average absorbed dose. By applying the dose reciprocity theorem (Brownell et al., 1968), the specific absorbed fraction at the center of a uniform distribution of activity can be calculated by dividing the appropriate central point source absorbed fraction by the target mass. The dose reciprocity theorem states that the absorbed dose delivered to a point from a uniform-volume distribution of activity is equal to the average absorbed dose delivered to that volume by the same

amount of activity concentrated at that point. This was the basis for computing the central point dose in the cylinders.

In all procedures, a pre-irradiation annealing cycle, as proposed by Cameron et al., (1964) has been used. This method is to anneal the dosimeters in an oven at 400°C for one hour. This empties all the traps in the lithium fluoride. The dosimeters are cooled 20 minutes to room temperature before being placed in another oven for 24 hours at 80°C. This anneal lets the traps arrange themselves so the 190°C peak predominates and the low temperature traps contribute as little as possible at readout. Also to lower the contribution from the low energy traps, the readout procedure recommended by Eberling Instrument Company (1967) was used. It incorporates a 140°C pre-heat anneal before readout.

Background was subtracted and all dosimeters in a batch were readout at the same time.

7.3 Air Calibration

The micro-dosimeters were also calibrated in air to find the response to the technetium-99m photons. This was then compared to the response from cobalt-60. Technetium-99m is commonly quoted as having a specific gamma ray constant of 0.56 R-cm^2/mCi-hr @ 1 cm. However, one must consider the 18.3 KeV K X-rays from the internal conversion process which adds 0.02 R-cm^2/mCi-hr @ one cm. The 20.6 KeV K X-rays from internal conversion adds another 0.12 R-cm^2/mCi-hr @ one cm. This makes the specific gamma ray constant for

technetium-99m 0.70 R-cm^2/mCi-hr @ one cm (Smith, 1964).

The dosimeters were held ten cm from a plastic tube containing ^{99m}Tc precipitate. The precipitate occupied a volume of less than one-half ml in a thin rounded bottom plastic vial. This arrangement approximated a point source. The dosimeters were held at ten cm on both sides of the vial by cellophane tape.

At ten cm less than one percent of the exposure was attenuated by air. The amount of attenuation from the glass wall and the thin wall of the plastic vial was also small. These factors were considered in the air calibration of the dosimeters.

7.4 Experimental Procedures

The lung scanning agent used was developed by Ficken (1970). The agent was a technetium-99m labelled sulfur macro-aggregate. The sulfur macro-aggregate (SMA) was prepared in the Nuclear Medicine laboratory of the Hospitals of the University of Oklahoma Health Sciences Center. To prepare the agent, a vial containing technetium-99m was brought to a volume of 4½ ml by the addition of saline. To this one ml of a mixture of gelatin, sodium perrhenate, and sodium thiosulfate was added. One ml of HCl was added and the solution was heated 15 minutes in an oil bath at 100°C. Then two ml of buffer and one ml of gluteraldehyde solution were added. This mixture was placed in the 100°C oil bath and vigorously shaken for three minutes. The agent was then washed twice

and a particle size determination made. A culture to check for sterility is made if the agent is used for humans. The agent was injected through an 18 gauge needle slowly to prevent particle breakup.

For a human scan, the injected agent contains one to three million aggregates with a size distribution between five and thirty microns in diameter. Aggregates of this size will lodge in the lung vasculature on the first pass through the lung. The particles that are too small to lodge in the lung are trapped by the liver. The injection of smaller particles than those used in lung scans, that pass through the lung, is the basis for the liver scan.

In this study, mongrel dogs of the size range of 15 to 25 kilograms were used. The dogs were anesthetized with sodium pentobarbital at the rate of one ml per five pounds of body weight. Sodium pentobarbital was used instead of nebutal to give a two to three hour period of complete anesthesia. This allowed a period of time sufficient to raise the jugular vein, inject the scanning agent, inject the dosimeters, tie off the jugular, and to close the incision where the jugular was raised. After the jugular was tied off, the jugular on the opposite side of the body was able to carry the total blood flow satisfactorily. There was then time to transport the dog to do a lung scan and to get him back to the animal compound before the anesthesia was gone.

The scanning agent was introduced into the cephalic vein of the foreleg. The left or right jugular was raised and positioned to introduce the dosimeters immediately after the injection of the scarning agent. The reason for introducing the dosimeters after the scanning agent was because of the larger size of the dosimeter. They could block the precapillary area of the lung. This blockage would prevent the scanning agent from getting into the capillary areas of the lung vasculature and would lead to a poor distribution of the scanning agent. Also, this could cause an erroneously high dosimeter reading because the particles would be in direct contact with the dosimeters.

The amount of isotope injected depended upon the dose desired to the lung. In internal studies of this type, it was acceptable to inject much more agent than in a human scan improving the dosimeter accuracy. For a human scan five millicuries is used with technetium-99m labelled aggregates. We used about 50 mCi per dog.

Studies by Darnell (1967) indicate that the anatomical position of the dog will change the distribution of the scanning agent and of the injected dosimeters. Studies by Glazier (1967) also state that gravity and, thusly, body position will cause differences in regional blood flow. This pointed out the need for a uniform injection position for both injecting the lung scanning agent and the subsequent dosimeter insertion.

The exact position of the animal was determined at the time of the procedure. This was dictated by the surgical procedures necessary to expose the jugular vein needed to insert the dosimeters. Approximately twenty dosimeters were used per dog. This was approximately one dosimeter for every ten grams of lung tissue. It also must be remembered that since the jugular was tied off after the insertion of the dosimeters, an adequate flush of saline was needed to get them to the heart to be pumped into the lung.

7.5 Recovery of Dosimeters

Twenty four hours after the injection of the scanning agent, and the insertion of the dosimeters, the dog was sacrificed. This was accomplished by using twice the dose of sodium pentobarbital, as used for anesthesia. This was a very humane death.

At the time of death the lungs were removed. Many of the dosimeters could be found in the lung tissue by palpatation. The remaining dosimeters were recovered using an acid digestion of the remaining lung tissue. On some of the dogs, each lobe of the lung was removed and separately digested to get the distribution of the dosimeters in the lung.

7.6 Effective Half-Life Determination

The need for exact determination of the effective half-life in the lung of the agent was of prime importance in the calculation and measurement of absorbed dose to the lung. After the lung scanning agent was injected, the animal was

placed under an Anger camera and counts were made at thirty minute intervals through two effective half-lives. The results were plotted and the effective half-lives determined. During the counting times, the liver and spleen area was shielded with a lead sheet to prevent the activity in the liver and spleen from interfering with the decreasing lung activity.

7.7 Dose From Liver To Lung

After the scanning agent is injected into the lung, some of the agent begins to be removed by several processes to the liver and spleen. This can contribute a significant dose to the lung. To determine the dose to the lung from the agent in the liver, a technetium-99m sulfur macroaggregated liver scanning agent was injected. The dose from the liver agent to the lung was recorded on dosimeters injected into the lung.

By correcting this measured number for the rate of uptake by the liver, we can subtract this value from the measured lung dose to get the value of dose to the lung from the agent in the lung (the case of self-irradiation).

CHAPTER VIII

EXPERIMENTAL RESULTS

8.1 In Vitro Measurements

To analyze the results of the dog lung measurements, it was necessary to calibrate the dosimeter response per rad to technetium-99m photons relative to cobalt-60 response per rad. This was done by computing the dose delivered to the central point of cylinders of ten cm in diameter and five, ten, and twenty cm in height. The central point absorbed fractions for these cylinders were taken from data compiled by Brownell et al., (1968). The method of calculation is identical to the calculation of lung dose. The measured value of dose agrees with the calculated gamma dose plus increased response due to the low energy component. This data supports the fact that the beta like radiations were not measured due to the glass encapsulation of the lithium fluoride powder.

The 20 cm high cylinder was found to give an over response of 33 $\pm$ 4%, as compared to the response per rad of cobalt. It should be noted that the error figures are given as $\pm$ one standard deviation from the mean. As the height of the cylinders was decreased, the relative over response was also found to be decreased. This was because fewer degraded photons reached the dosimeters. It should be mentioned that the mean free path of a 140 KeV photon is 6.67 cm in unit density tissue (Ellett and Humes, 1971).

At a cylinder size of five cm in height and ten cm in diameter, the over response was found to be about five percent. The 375 gram mass of the cylinder is a very rough approximation of the 270 gram dog lung. The air over response was found to be about seven percent. The values for the measured over response vs. mass are shown in figure 8.1

From the data, it would be expected that the over response value for a mass the size of a dog lung would be approximately five percent as compared to cobalt-60. This factor of five percent was used to correct the ^{60}Co calibrations for the increased response of lithium fluoride to low energy photons. A typical TLD calibration is shown in the appendix, Table A.

8.2 TLD Recovery

The dosimeters were recovered from the lung tissue by palpatation and acid digestion of the lung tissue. The recovery pattern of four dogs is shown in Table 2. The lung was removed and each lobe of the lung placed in a beaker for acid digestion to find the number of dosimeters in each lobe.

Two of the dogs had the left jugular raised and the other two had the right jugular raised. By raising the jugular and turning the head while inserting the dosimeters, there was a definite downside lung. This lead to a high percent of dosimeters in the downside lung. But when all dogs were considered it was shown that there was nearly an even distribution. During the course of the experiment one-half of the

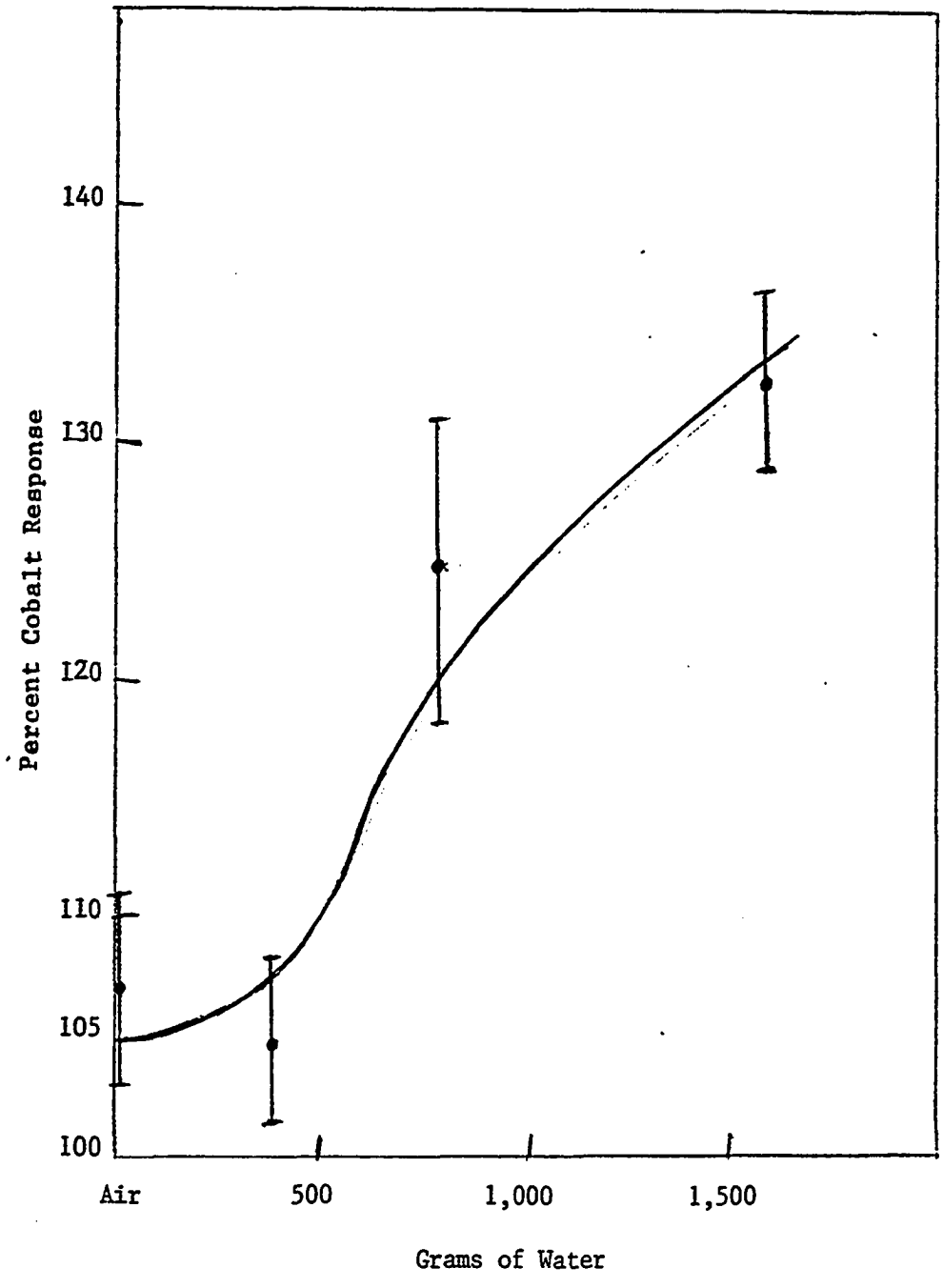

Figure 8.1 Technetium-99m Over Response

Table 2. Dosimeter Location

Left Jugular Raised

Left Lung			Right Lung		
Dog number	1	2		1	2
Apical	0	0	Apical	1	7
Cardiac	2	1	Cardiac	13	5
Diaphagmatic	2	2	Diaphagmatic	0	3
			Intermediate	0	0
Total	4	3		14	15

Right Jugular Raised

Left Lung			Right Lung		
Dog number	3	4		3	4
Apical	10	6	Apical	0	0
Cardiac	1	3	Cardiac	0	0
Diaphagmatic	5	2	Diaphagmatic	0	0
			Intermediate	0	2
Total	16	11		0	2

Total recovery on four dogs;

Right Lung	34
Left Lung	31

dogs had dosimeter insertion on the right, and the other half on the left. This was done to average the effects of the downside lung when the dosimeters were injucted.

8.3 Half-Life Determination

The effective half-life of the lung scanning agent was determined by plotting count rates of the activity over the lungs. Counts were taken at 30 minute intervals through two effective half-lives. The effective half-life was found to be 2.7 ± 0.5 hours. A typical half-life determination is shown in the appendix, Table A.

8.4 Dose From Liver To Lung

Some of the dose to the lung tissue results when the labelled aggregate is cleared from the lung into the liver and spleen primarily (Ficken, 1970). In the human, the liver dose to the lung from the lung scanning agent will contribute 12 mr/mCi injected (Synder et al., 1969). The calculated human lung dose was 63 mr/mCi. This shows that This shows that about 20% more dose is received by the lung from the agent going to the liver.

The dose from the liver to the lung was found by injecting two dogs with liver scanning agent and then inserting the TLD's into the lung. The dose to the lung from the liver was found to be 63 mr/mCi to the lung, but due to a longer uptake time of the lung agent by the liver, the dose to the lung from the liver by the scanning agent was found to be 34.7 ± 16 mr/mCi. This calculation is shown in the appendix, Table B.

8.5 In Vivo Measurements

In the course of this experiment, 11 mongrel dogs were used. The dogs weight ranged from 11.8 to 24.3 kilograms with an average weight of 18.5 kilograms. The dogs were injected with between 25 and 75 millicuries of technetium-99m labelled sulfur macroaggregated lung scanning agent. Lung scans showed that the agent was lodged in the lung. A typical lung scan is shown in figure 8.2.

Ninty-five percent of the amount injected was assumed to lodge in the lung, the other five percent goes through the lung into the liver (Ficken, 1970). These figures were the basis of the measured gamma dose to the lung per millicurie. The average measured gamma dose to the lung was found to be 180 $\pm$ 15 millirad per millicurie lodged in the lung. This data is shown in Table 3. A typical measurement is shown in the appendix, Table A.

8.6 Calculation of Lung Dose

The calculation of the dose to the lung of standard man was outlined in Chapter VI. This calculation was for both the beta like and the gamma absorbed dose. In this study, the beta like radiations were not measured due to the type of dosimeter used. The gamma dose reflects only 28.7% of the total value or 63.1 millirad per millicurie injected.

These calculations assume instantaneous uptake of the

Figure 8.2 Dog Lung Scintiphoto

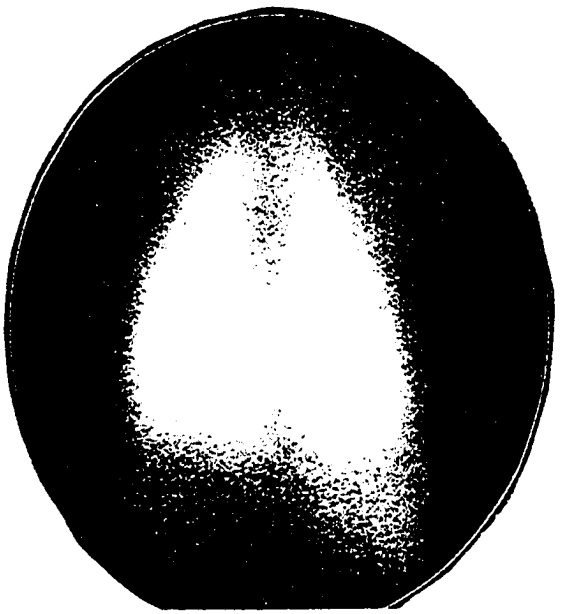

Table 3. Measured Dog Lung Gamma Dose

Weight Kg	TLD's recovered	mCi injected	rads	mrad/mCi	T_{eff} hours
16.5	10	72.5	14.0 ± 0.7	191	
11.8	14	40.6	9.0 ± 0.8	223	
13.7	20	43.4	13.2 ± 0.6	304	
19.7	4	52.0	7.8 ± 1.3	148	
20.4	19	46.5	9.0 ± 0.5	193	
24.3	19	65.4	11.0 ± 0.7	168	
19.5	15	26.4	3.1 ± 0.5	118	1.45
20.0	14	34.7	7.1 ± 0.8	205	4.15
16.8	11	38.2	4.7 ± 0.6	124	2.25
20.4	18	55.8	12.9 ± 1.1	231	3.55
20.4	18	57.8	9.7 ± 0.7	167	2.05

The data is corrected to reflect $^{99m}Tc = 1.05\ ^{50}Co$.

Average dog weight = 18.5 Kg

Effective half-life = 2.7 ± 0.5 hours

Average gamma dose = 180.5 ± 14.7 mrad/mCi.

labelled aggregates and instantaneous implantation of the dosimeters in the lung. Corrections were needed for these times and were dictated by the time involved at the time of the experiment. It must be remembered that these percentages were calculated for standard man. Also, the calculated dose shown in Chapter VI was for the case of self irradiation of the lung by the scanning agent.

Since no Monte Carlo calculation was available for a lung the size of the dog, another method of abtaining absorbed dose was needed. The method used was to take the tabular values of absorbed fraction corresponding to mass m in a unit-density medium, which will correspond to a mass of m/ρ^2 in a medium of density ρ (Brownell et al., 1968). The density transformation rule states that all parameters with dimensions in which mass and length occur as an intergral of (mass / length^2), are independent of mass density, provided that the distance between all pairs of points in or on the surface of each region is constant in terms of mass per unit area (Loevinger and Berman, 1968). This means that if the volume is defined such that the distance from the source to every point of the volume is constant in g/cm^2 , then the absorbed fraction is independent of density, and the mass is inversely proportional to the density squared. The lung has a density of 0.32 g/cc. The tabular values in the table will then

increased by a factor of about ten($m/\rho^2 = m/0.1 = 10m$). The results of these gamma dose calculations are summarized in Table 4.

Using the conversion, the tabulated values of absorbed fraction for human lung was found. In this case, a flat ellipsoid of a mass of 1,000 grams and a density of 0.32 (which corresponds to a 100 gram mass unit density material) was assumed to be equivalent to the human lung. The dose was found to be 68.2 mrad/mCi. This value is in reasonable agreement with the 63.1 mrad/mCi calculated from the more refined Monte Carlo technique discussed previously.

The same method was employed using absorbed fraction values for a unit density ellipsoid of a mass of 26 grams for calculating the dose to the dog lung.

The weight of the dog lung in the calculation was based on the assumption that the lung weighs 1.4% of body weight. The average dog weight was 18.5 kilograms. This gives an estimated lung weight of 259 grams. This calculation gives a dose of 127 mrad/mCi. The effective half-life was found to be 2.7 ± 0.5 hours. This value was used in the calculation of the dog lung gamma dose.

The doses were calculated using tables of absorbed fractions with a backscatter medium surrounding the volumes of interest. These values are published by the MIRD (Ellett and Humes, 1971) and are for flat ellipsoids with a principle axis ratio of one to two to four. The flat ellipsoid more

Gamma	$\bar{E}_i$	Δ_i	Human ϕ	Human $\phi\Delta_i$	100 g ellipsoid ϕ	100 g ellipsoid $\phi\Delta_i$	26 g ellipsoid ϕ	26 g ellipsoid $\phi\Delta_i$
1	0.0021	0.0000	1.0000	0.0000	1.0000	0.0000	1.0000	0.0000
2	0.1405	0.2643	0.0496	0.0131	0.0530	0.0140	0.0270	0.0072
3	0.1427	0.0001	0.0496	0.0000	0.0530	0.0000	0.0270	0.0000
X-rays								
K_α-1	0.0184	0.0017	0.5100	0.0009	0.4500	0.0012	0.4000	0.0007
K_α-2	0.0183	0.0008	0.5100	0.0004	0.4500	0.0004	0.4000	0.0003
K_β-1	0.0206	0.0005	0.4750	0.0002	0.4500	0.0002	0.4000	0.0002
K_β-2	0.0210	0.0001	0.4750	0.0001	0.4500	0.0001	0.4000	0.0000
L	0.0024	0.0000	1.0000	0.0000	1.0000	0.0000	1.0000	0.0000
			$\Sigma\phi\Delta_i$ = 0.0146		$\Sigma\phi\Delta_i$ = 0.0158		$\Sigma\phi\Delta_i$ = 0.0084	

Human Lung (self irradiation) $1.44 \times \frac{1{,}000\,\mu Ci}{1{,}000\ g} \times 3\ hr \times 0.0146 = 0.0631\ rad = 63.1\ mr/mCi.$

Human (as 100 g ellipsoid) $1.44 \times \frac{1{,}000\,\mu Ci}{1{,}000\ g} \times 3\ hr \times 0.0158 = 0.0682\ rad = 68.2\ mr/mCi.$

Dog (as 26 g ellipsoid) $1.44 \times \frac{1{,}000\,\mu Ci}{259\ g} \times 2.7\ hr \times 0.0084 = 0.1270\ rad = 127\ mr/mCi.$

Table 4 Calculation of Dose

closely approximates the lung than that of other common geometric s hapes.

8.7 Calculated and Measured Dose

The gamma dose to the dog lung was calculated to be 127 mrad/mCi. The measured gamma dose to the lung was 180.5 ± 14.7 mrad/mCi. The dose contributed to the lung from the liver was found to be 34.7 ± 16 mrad/mCi. This gives a gamma dose to the dog lung of 145.8 ± 22 mrad/mCi for the agent in the lung giving a dose to the lung.

8.8 Discussion of Errors

The standard deviation of the mean of the thermoluminescent dosimeter readings on a typical cobalt calibration was found to be 6.5% (a dose of approximately 50 rads). The standard deviation of the mean of the TLD's used in a typical dog run was found to be 6.4% of the mean with a dose of ten rads. Thus, the Tld standard error was found to be $\sqrt{(6.4)^2 + (6.5)^2} = 9.2\%$ in this particular run.

Another major source of variation in this experimental value was the biological variability between the dogs. This variation was undoubtedly, also, reflected in the 8.1% standard deviation of the mean of the measured dose of 180 mrad/mCi. The range in the measured dog lung dose was from 118 to 304 mrad/mCi.

When comparing the calculated value of 127 mrad/mCi to the measured value of 145.8 mrad/mCi, several factors should be considered. It should first be recognized that the

measured dose is approximately 15% higher than that of the gamma dose calculation using the method and tabular values of absorbed fractions of MIRD for an ellipsoid the size of the dog lung surrounded by a scatter medium.

A source of systematic error that must be considered in the calculation is that the lung weight of the dog was estimated at 1.4% of body weight. Error in this value will change the calculated dose inversely to a weight change. Tenny (1963) has found that between species the lung volume is proportional to lung weight. The factor 1.4% was used because the 70 kilogram standard man has a lung weight of 1,000 grams, which is 1.4% of body weight. The lung weights were not measured in this experiment due to the many problems involved in doing this accurately. Several factors such as the type of death, how much blood is lost, deflation, etc., may cause erroneous values for the measured weight of the lung.

Another source of error in computing the lung dose arises from the fact that the method used for the dog lung assumes that the shape is that of a flat ellipsoid using a density correction. In the human lung calculation, the values obtained using the ellipsoidal calculation and the Monte Carlo calculation differ by about eight percent. The flat ellipsoid is not as accurate as the full Monte Carlo technique, but in the case of the dog lung, it was the best available method.

A possible measurement error could result from an over response which may be larger than the five percent used to calculate the rad dose. Lithium fluoride can have an over response to low energy photons as large as 40% as compared to cobalt-60 (Cameron, 1968). This can also be seen in figure 8.1 for the water calibration. For these measurements, there was little backscatter material, which would be most accurate if the dog lung were outside the body, but due to the body surrounding the lung, this factor may not be correct. The degraded photons being scattered back to the dosimeters could be a reason for the dosimeter sensitivity per rad being larger than was used. With the difficulties of determining lung weight and size, a more accurate assessment of this correction was not attempted.

The effect of the large variance in the biological half-life would lead to a discrepancy between experimental and theoretical values. If the agent were to reside in the lung longer than expected, this would increase the effective half-life. If the effective half-life were to approach the six hour physical half-life, i.e., if the agent remained in the lung indefinitely, a doubling of the absorbed dose would occur.

The biological half-life of the agent was found to be 4.9 hours (effective half-life of 2.7 ± 0.5 hours). Ficken (1970) found a six hour biological half-life for this agent by labelling the sulfur macroaggregate with ^{35}S. DeLand

(1966) has found the biological half-life of the macro-aggregated albumin lung scanning agent to range from four to 12 hours with a mean of eight hours. Furth et al., (1965) have reported six hours as the biological half-life, and Abiston and Wagner (1964) report clearance half-lives from three to seven hours. It should be pointed out that all of these numbers are not for the same agent. Nevertheless, it is evident that there is variability in the data on biological half-lives.

CHAPTER IX

CONCLUSIONS

The measurement of the gamma dose to the lung from technetium-99m labelled lung scanning aggregates was found to be 145.8 ± 22 mrad/mCi. This compares to a calculated value of 127 mrad/mCi. In an earlier in vivo study by Darnell (1967), a value of total dose of 70 mrad/mCi was measured.

In considering the previously mentioned factors in assessing the calculated and measured dose by using the best available factors, we must conclude:

1. There is no significant difference between the calculated and the measured gamma dose at the 95% level of significance.
2. The high variability of half-life shows that the individual dose can deviate greatly from the mean.
3. There is an uncertainty in the backscatter from surrounding tissue that needs to be more accurately assessed. This also affects the quality of radiation that strikes the dosimeter.
4. The dose to the liver and spleen is significant and contributes significantly to the total lung dose.
5. The micro-TLD's can be used to get acceptable results in vivo.

APPENDIX

Table A. Typical Measurement and Calculation

Dosimeter Calibration

The dosimeters were exposed in a phantom to a 10 X 10 cm field @ 80 cm SSD for 20 seconds. The shutter error was - 0.6 seconds. The following equation gives a dose in rads:

152.5 R/min X 0.882 decay correction X 0.966 R to rad X 1.035 backscatter factor X $\frac{19.4 \text{ sec.}}{60 \text{ sec/min}}$ = 43.5 rads.

TL readout				Background TL		
1	498	10	495	1	8	
2	690	11	765	2	19	
3	384	12	384	3	26	
4	662	13	409	4	28	
5	391	14	532	5	28	
6	520	15	422	6	26	
7	485	16	507	7	28	
8	610	17	322	8	27	
9	769	18	343	9	20	
		$\bar{X}$ =	510.4	10	21	$\bar{X}_{bkg}$ = 23

510.4 - 23 = 487.4 TL $\qquad \frac{487.4 \text{ TL}}{43.5 \text{ rad}}$ = 11.2 TL/rad

Dog # 11 TL of recovered dosimeters

1	94	10	127
2	154	11	121
3	127	12	130
4	142	13	106
5	173	14	150
6	184	15	187
7	105	16	78
8	88	17	173
9	131	18	broken

The dog was injected with 60.9 mCi with a 95% uptake to the lung.

$\bar{X}$ = 133.5 133.5 - 23 (bkg) = 113.5 TL

$\frac{113.5 \text{ TL}}{1.05 \text{ over response}}$ = 108.1 corrected TL

$\frac{108.1 \text{ TL}}{11.2 \text{ TL/rad}}$ = 9.65 rad dose to the lung

$\frac{9.65 \text{ rad}}{57.8 \text{ mCi}}$ = 167 mrad/mCi

Dosimeter recovery pattern

Left jugular raised

Left Lung		Right Lung	
Apical	0	Apical	7
Cardiac	1	Cardiac	5
Diaphagmatic	2	Diaphagmatic	3
		Intermediate	0
Totals	3		15

Effective Half-Life Counts

Time (hours)	Counts
0.0	1,000,214
0.5	948,619
1.0	802,374
1.5	667,432
2.0	578,122
2.5	480,530
3.0	403,026
3.5	336,280

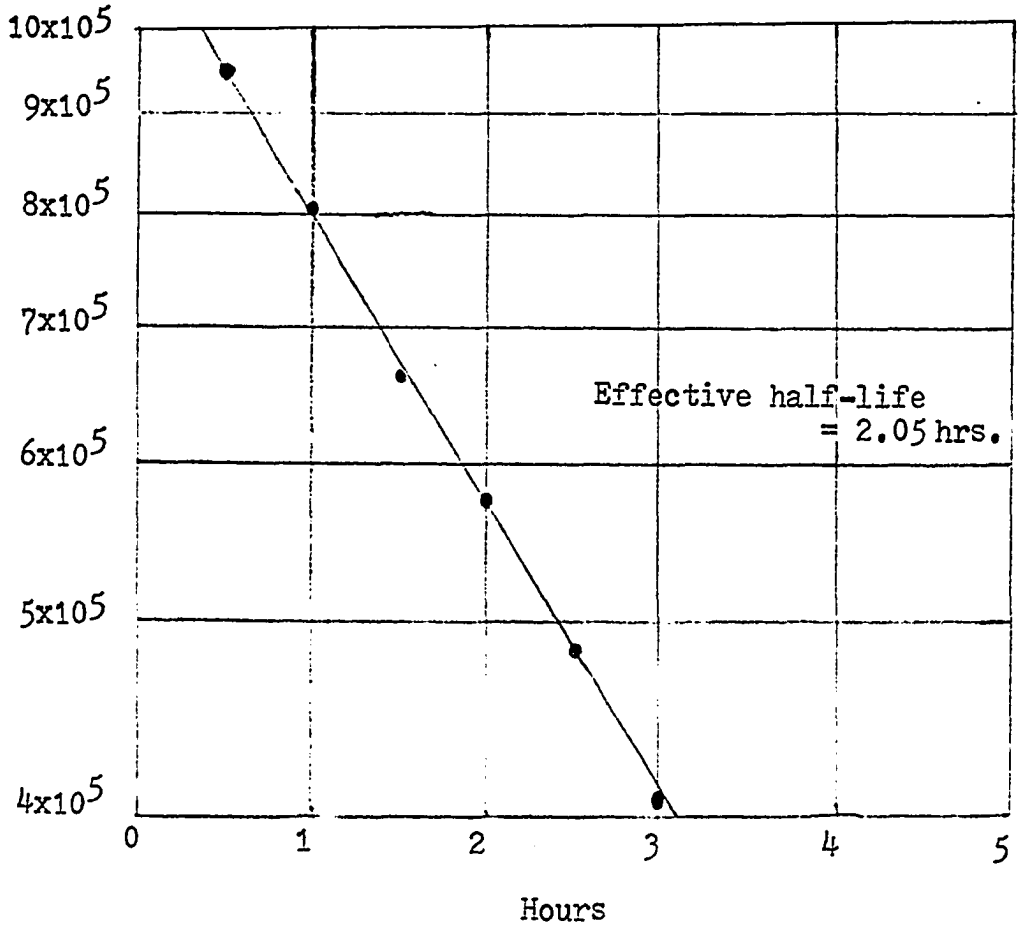

Table B Dose From Liver to Lung

TL readout	
1	53
2	92
3	22
4	81
5	51
6	42
7	56
8	66
9	29
10	29
11	24
12	28
13	28
14	33
15	21
16	26

$\bar{X}$ = 42.6 bkg = 13.4

42.6 - 13.4 = 29.2 TL Cobalt cal. = 12.8 TL/ rad

$\frac{29.2 \text{ TL}}{12.8 \text{ TL/rad}} = 2.28$ rad $\frac{2.28 \text{ rad}}{1.05 \text{ over response}} = 2.17 \pm 0.41$ rad

Five percent of the liver agent was held in the lung or 1.3 mCi.

1.3 mCi X 180 mrad/mCi (measured lung dose) = 0.23 rad

2.17 rad - 0.23 rad = 1.94 $\pm$ 0.41 rad

26.3 mCi injected - 1.3 mCi in lung = 25 mCi to liver

This gives a dose to the lung of 78 $\pm$ 16 mrad/mCi. The rate of uptake by the liver of the lung agent is governed by the effective half-life of the lung agent. The effective concentration in the liver of the lung agent would be reduced by (1 - T_{up} / T_{eff}). T_{up} = 2.7 hours, T_{eff} = 6 hours. 78 mrad/mCi X 0.55 = 42.9 mrad/ mCi dose from the lung agent in the liver to the lung.

BIBLIOGRAPHY

Adolph, E.F., Science, 109 (1949) p. 579.

Aitken, M.J., Reid, J., Tite, M.S., and Fleming, S.J., "Quenching of Spurious Thermoluminescence by Nitrogen", Luminescence Dosimetry, Proc. of Int. Conf., Stanford, Calf., A.E.C. Symposium Service, Vol. 8, CONF 650637 USAEC (9167) pp. 236-243.

Beck, W.L., Callis, E.L., and Cluotier, R.J., "Phantom Depth-Dose Measurements with Extruded LiF in a Low-Exposure-Rate Total-Body Irradiator", Proceedings of the Second International Conference on Luminescence Dosimetry, CONF-68921 (1968) pp. 976-989.

Berger, M.J., "Distribution of Absorbed Dose Around Point Sources of Electron and Beta Particles in Water and Other Media", MIRD Pamphlet No. 7, J. Nuclear Medicine, Suppl. No. 5, 1971.

Bloomer, W.E., Liebow, A.A., and Hales, M.R., Surgical Anatomy of the Bronchovascular Segments, Thomas, Springfield, Ill. 1960.

Boone, M.L., Jardine, J.H., Wright, A.E., and Taphy, N., "High-Energy Electron Dose Perturbations in Regions of Tissue Heterogenity, Part I In Vivo Dosimetry", Radiology, Vol.88 No. 6 (1967) pp. 1136-1145.

Brewer, N.R., "Housing for Research Dogs", Federal Proceeding, 20 (1961) p. 917.

Brownell, G.L., Ellett, W.H., and Reddy, A.R., "Absorbed Fractions for Photon Dosimetry", MIRD Pamphlet No. 3 J. Nuclear Medicine, Suppl. No. 1, 15, 1968.

Burlin, T.E., "Cavity-Chamber Theory", Radiation Dosimetry, Chapter 8, Vol. I, Second Edition, Edited by F.H. Attix and W.C. Roesch, Academic Press, New York, 1968.

Bush, F., "The Integral Dose Received From a Uniformly Distributed Radioactive Isotope", British J. of Radiology, 22 (1949) p. 96.

Cameron, J.R., Suntharalingam, N., and Kenny, G.N., Thermoluminescent Dosimetry, The University of Wisconsin Press, Madison, 1968.

Cass, J.S., "Control of Quality in Laboratory Animals to Increase Effectiveness of Biological Research", Federal Proceedings, 20 (1961) p. 907.

Darnell, T.C., "In Vivo Dosimetry in the Lung for Internally Administered Radioactive Isotopes", Dissertation, University of California at Los Angelos, 1967.

DeLand, F.H., "The Fate of Macroaggregated Albumin Used in Lung Scanning", J. Nuclear Medicine, 7 (1966) pp. 883-895.

DeReuck, A.V.S., and O'Connor, M., Ciba Foundation Symposium on Pulmonary Structure and Function, Little, Brown and Co., Boston, 1962.

Dillman, L.T., "Radionuclide Decay Schemes and Nuclear Parameters for Use in Radiation-Dose Estimation", MIRD Pamphlet No. 4, J. Nuclear Medicine, Suppl. No. 2, 1969.

Duffy, G.J., DeNards, G., and Abington, R.B., "Origin and Evolution of Radioactive Pulmonary Emboli in Man", Radiology, 91 (1968) pp. 1175-1180.

Eberline Instrument Company, "TLD Reader Model TLR-5 Technical Manual", 1969.

Ellett, W.H., Callahan, A.B., and Brownell, G.L., "Gamma-Ray Dosimetry of Internal Emitters-Monte Carlo Calculation of Absorbed Dose From Uniform Sources", British J. of Radiology, 1965.

Ellett, W.H., Callahan, A.B., and Brownell, G.L., "Gamma-Ray Dosimetry of Internal Emitters-Monte Carlo Calculations of Absorbed Dose From Point Sources", British J. of Radiology, 37 (1964) pp. 37-45.

Ellett, W.H., Callahan, A.B., and Brownell, G.L., "Gamma-Ray Dosimetry of Internal Emitters", British J. of Radiology, 38 (1965) pp. 541-544.

Ellett, W.H., and Humes, R.M., "Absorbed Fractions for Small Volumes Containing Photon-Emitting Radioactiviy", MIRD Pamphlet No. 8, J. Nuclear Medicine, Suppl. No. 5, March 1971.

Endres, G.W.R., Kalhren, R.L., and Kocher, L.F., " Thermoluminescence Personnel Dosimetry at Hanford-II. Energy Dependence and Application of TLD Materials in Operational Health Physics", Health Physics, 18 (1970) pp. 665-672.

Engel, S., Lung Structure, Thomas, Springfield, Ill., 1962.

Ficken, V.J., "A New Lung Scanning Agent", Thesis, University of Oklahoma, 1970.

Focht, E.F., Quimby, E.H., and Gershowitz, M., "Revised Average Geometric Factors for Cylinders in Isotope Dosage. Part I", Radiolody, 85 (1965) p. 151.

Fowler, J.F., and Attix, F.H., "Solid State Integrating Dosimeters", Radiation Dosimetry, Chapter 13, Vol. II Second Edition, Edited by F.H. Attix and W.C. Roesch, Academic Press, New York, 1966.

Furth, E.C., Okenak, A.J., Focht, E.F., and Becker, D.V., "The Distribution, Metabolic Fate and Radiation Dosimetry of I-131 Labelled Macroaggregated Albumin", J. Nuclear Medicine, 6 (1966) pp, 506-518.

Harshaw Chemical Company, 1971 Private Communication.

Johns, H.E., and Cunningham, J.R., The Physics of Radiology, Third Edition, Charles C. Thomas, Springfield, Illinois, 1969.

Kastner, J., Hukkoo, R., and Oltman, B.G., "Lithium Fluoride Thermoluminescent Dosimetry for Beta Rays", Luminescence Dosimetry, Proc. Int. Conf., Stanford, Calf. AEC Symp. Serv., Vol. 8, CONF 650637, USAEC (1967) p. 482.

Loevinger, R., and Berman, M., "A Schema for Absorbed-Dose Calculations for Biologically-Distributed Radionuclides", MIRD Pamphlet No. 1, J. Nuclear Medicine, Suppl. No. 1, 1968.

Lucas, A.C., French, N.R., "A Minature Thermoluminescent Dosimeter and Its Application in Radioecology", Luminescence Dosimetry, Proc. Int. Conf., Stanford, Calf., AEC Symp. Serv., Vol. 8, CONF 650637, USAEC (1967) p. 402.

Mason, Marcus M., "Bibliography of the Dog", The Iowa State University Press, Ames, Iowa, 1959.

Quimby, E.H., Feitelberg, S., and Gross, W., "Radioactive Nuclides in Medicine and Biology, Third Edition, Lea and Febiger, Philadelphia, 1970.

Reddy, A.R., Ellett, W.H., and Brownell, G.L., "Gamma-Ray Dosimetry of Internal Emitters III - Absorbed Fractions For Low Energy Gamma-Rays", British J. of Radiology, 40 (1967) p. 512.

Robbins, P.J., and Fortman, D.L., "A Kit for Technetium-99m Macroaggregated Albumin", Nuclear Medicine Technical Note, U.S. Dept. of Health, Education, and Welfare, 1971.

Ross, R.B., "Influence of Bronchial Tree Structure on Ventilation in the Dog's Lung as Inferred From Measurements of a Plastic Cast", J. Appl. Physiol., Vol. 10 (1957) pp. 1-14.

Sabiston, D.C., and Wagner, N.H., "The Diagnosis of Pulmonary Embolism by Radioisotope Scanning", Ann. Surg., 160 (1964) pp. 575-585.

Schmidt-Nielsen, B., "Choice of Experimental Animals for Research", Federal Proceedings, 20 (1961) pp. 902-906.

Schulman, J.H.," Survey of Luminescence Dosimetry", Luminescence Dosimetry, Proc. Int. Conf., Stanford, Calf, AEC Symp. Serv., Vol. 8, CONF 650637, USAEC (1967) pp. 3-33.

Smith, E.M., "Calculating Absorbed Doses From Radiopharmaceuticals", Nucleonics, 24 (1966) p. 35.

Smith, E.M., "Internal Dose Calculation for Technetium-99m", J. Nuclear Medicine, 6 (1965) pp. 321-351.

Smith, E.M., "Properties, Uses, Radiochemical Purity, and Calibration of ^{99m}Tc", J. Nuclear Medicine, 5 (1964) pp. 871-882.

Snedecor, G.W., and Cochran, W.G., Statistical Methods, Sixth Edition, The Iowa State University Press, Ames Iowa, 1968.

Snyder, W.S., and Ford, M.R., "Estimates of Absorbed Fractions for Monoenergetic Photon Sources Uniformly Distributed in Various Organs of a Heterogenous Phanton", MIRD Pamphlet No. 5, J. Nuclear Medicine, Suppl. No. 3, 1969.

Spuring, J., Novoting, J., and Hedvicakova, L., "Thermoluminescent Dosimetry Using Lithium Fluoride in Aqueous Suspensions", Phys. Med. Biol., Vol. 16, No. 2 (1971) pp. 295-301.

Tenney, S.M., and Remmers, J.E., "Comparative Quantitative Morphology of the Mammalian Lung: Diffusing Area", Nature, Vol. 197 (1963) pp. 54-56.

Tow, D.E., Wagner, H.N Jr., Lopes-Majano, V., Smith, E.M., and Migita, T., "Validity of Measuring Regional Pulmonary Arterial Blood Flow with Macroaggregates of Human Serium Albumin", Am. J. Roent. and Rad. Therapy, 96 (1966) pp. 664-676.

Trucco, E., "Self Absorption in Spheres and Cylinders of Radioactive Materials", Bulletin of Mathematical Biophysics, 26 (1964) p. 96.

Tyler, W.S., McLaughlin, R.F., and Canada,R.O., "Structural Analogues of the Respiratory System", Arch. Environmental Health, 14 (1967) pp. 61-69.

Wagner, H.N., "Current Status of Lung Scanning", Radiology, 91 (1968) pp. 1235-1237.

Wagner, H.N., Principles of Nuclear Medicine, W.B. Saunders Co., Philadelphia, (1968).

Weibel, E.R., Morphometry of the Human Lung, Springer, Berlin, 1963.

Widman, J.C. and Pawsner, E.R., "Energy Absorption in Cylinders Containing Axial Sources", J. of Nuclear Medicine, 7 (1966) pp. 407-415.

Widman, J.C. and Powsner, E.R., "Energy Absorption in Cylinders Containing a Uniformly Distributed Source", J. of Nuclear Medicine, 8 (1967) pp. 179-186.

Zimmerman, D.W., Rhyner, C.R., and Cameron, J.R., "Thermal Annealing Effects on the Thermoluminescence of Lithium Fluoride", Health Physics, Vol. 12 (1966) pp. 525-531.